

UC San Diego

UC San Diego Previously Published Works

Title

IKK α negatively regulates ASC-dependent inflammasome activation.

Permalink

<https://escholarship.org/uc/item/48w3n4fp>

Journal

Nature communications, 5(1)

ISSN

2041-1723

Authors

Martin, Bradley N
Wang, Chenhui
Willette-Brown, Jami
[et al.](#)

Publication Date

2014-09-01

DOI

10.1038/ncomms5977

Peer reviewed



Published in final edited form as:

Nat Commun. ; 5: 4977. doi:10.1038/ncomms5977.

IKK α negatively regulates ASC-dependent inflammasome activation

Bradley N. Martin^{1,11,12}, **Chenhui Wang**^{1,12}, **Jami Willette-Brown**², **Tomasz Herjan**¹, **Muhammet F. Gulen**¹, **Hao Zhou**¹, **Katarzyna Bulek**¹, **Luigi Franchi**³, **Takashi Sato**⁴, **Goutham Narla**⁵, **Xiao-Ping Zhong**⁶, **James Thomas**⁷, **Dennis Klinman**⁴, **Katherine A. Fitzgerald**⁸, **Michael Karin**⁹, **Gabriel Nuñez**³, **George Dubyak**¹⁰, **Yinling Hu**², and **Xiaoxia Li**¹

¹Department of Immunology, Lerner Research Institute, Cleveland Clinic Foundation, Cleveland, OH 44195, USA

²Cancer and Inflammation Program, Center for Cancer Research, National Cancer Institute, Frederick, MD 21702, USA

³Department of Pathology, University of Michigan Medical School, Ann Arbor, MI 48109; and Comprehensive Cancer Center, University of Michigan Medical School, Ann Arbor, MI 48109, USA

⁴Laboratory of Experimental Immunology, National Cancer Institute, Frederick, MD 21702, USA

⁵Institute for Transformative Molecular Medicine, Department of Medicine, Case Western Reserve University, Cleveland, OH 44106, USA

⁶Departments of Pediatrics and Immunology, Duke University Medical Center, Durham, NC 27710, USA

⁷Department of Pediatric Medicine, Baylor College of Medicine, Houston, TX 77030, USA

⁸Division of Infectious Disease and Immunology, Department of Medicine, University of Massachusetts Medical School, Worcester, Massachusetts 01605, USA

⁹Laboratory of Gene Regulation and Signal Transduction, Departments of Pharmacology and Pathology, University of California San Diego, School of Medicine, 9500 Gilman Drive, San Diego, CA 92093, USA

¹⁰Department of Physiology and Biophysics, Case Western Reserve University School of Medicine, Cleveland, OH 44106, USA

Users may view, print, copy, and download text and data-mine the content in such documents, for the purposes of academic research, subject always to the full Conditions of use:http://www.nature.com/authors/editorial_policies/license.html#terms

Correspondence should be addressed to Xiaoxia Li (lix@ccf.org) and Yinling Hu (huy2@mail.nih.gov).

¹²These authors contributed equally to this work.

Author contributions

B.M., C.W., T.H., M.G., H.Z., and K.B., performed the *in vitro* experiments; J.W.-B. and T.S. performed the *in vivo* experiments; L.F., G.N., X.Z., J.T., D.K., K.F., M.K., G.N., and G.D. contributed reagents and helped to design the experiments; Y.H. contributed reagents, helped to design experiments, and helped to edit the manuscript; X.L. conceived the study, oversaw the experiments, analyzed the data, and wrote the manuscript.

Competing financial interests statement

The authors have no competing financial interests to declare.

¹¹Department of Pathology, Case Western Reserve University School of Medicine, Cleveland, OH 44106, USA

Abstract

The inflammasomes are multiprotein complexes that activate caspase-1 in response to infections and stress, resulting in the secretion of pro-inflammatory cytokines. Here we report that IKK α is a critical negative regulator of ASC-dependent inflammasomes. IKK α controls the inflammasome at the level of the adaptor ASC, which interacts with IKK α in the nucleus of resting macrophages in an IKK α kinase-dependent manner. Loss of IKK α kinase activity results in inflammasome hyperactivation. Mechanistically, the downstream nuclear effector IKKi facilitates translocation of ASC from the nucleus to the perinuclear area during inflammasome activation. ASC remains under the control of IKK α in the perinuclear area following translocation of the ASC/IKK α complex. Signal 2 of NLRP3 activation leads to inhibition of IKK α kinase activity through the recruitment of PP2A, allowing ASC to participate in NLRP3 inflammasome assembly. Taken together, these findings reveal a IKKi-IKK α -ASC axis that serves as a common regulatory mechanism for ASC-dependent inflammasomes.

Introduction

Inflammasomes are multiprotein complexes that contain a member of the nucleotide-binding domain leucine-rich repeat (NLR) or AIM2-like receptor (ALR) family, and are activated in response to a diverse range of microbial, stress and damage signals, triggering caspase-1 activation and resulting in maturation of the pro-inflammatory cytokines interleukin (IL)-1 β and IL-18¹⁻³. The NLRP3 inflammasome consists of NLRP3 linked via a homotypic pyrin domain (PYD) interaction to the inflammasome adaptor molecule apoptosis associated speck-like protein containing a C-terminal caspase-activation-and-recruitment (CARD) domain (ASC)^{4, 5}. ASC interacts with pro-caspase-1 via a CARD domain⁶. NLRP3 is activated by a wide range of pathogen-associated molecular patterns (PAMPS) and danger-associated molecular patterns (DAMPs), including the nucleoside adenosine triphosphate (ATP)⁷, nigericin⁷, double-stranded RNA⁸, monosodium urate (MSU) crystals⁹, and silica¹⁰⁻¹², among others.

Despite the diversity of potential activators, NLRP3 activation in bone marrow-derived macrophages (BMDMs) requires two distinct signals¹³. First, the cell must be “primed” by an NF- κ B-inducing ligand (signal 1), such as the toll-like receptor-4 (TLR4) ligand lipopolysaccharide (LPS), to increase the transcription/translation of inflammasome components, including NLRP3 and pro-IL-1 β ¹⁴⁻¹⁹. Several studies have demonstrated that other events also take place during this priming phase²⁰⁻²⁴, including the translocation of the inflammasome adaptor molecule ASC from the nucleus to the cytoplasm²³ and the deubiquitination of NLRP3^{20, 22}. Following priming, a second activator (signal 2) initiates the final assembly of the inflammasome complex. Rapid NLRP3 inflammasome formation in response to extracellular ATP is mediated by the purinergic receptor P2X7²⁵⁻²⁷.

While the inflammasome plays a critical role in host defense against microbial infections²⁸⁻³⁵, aberrant activation of the inflammasome has been implicated in the

pathogenesis of numerous human diseases^{36–40}. Therefore, the process of inflammasome activation is tightly controlled. However, the exact mechanism by which inflammasome activation is regulated has remained controversial and unclear. We became interested in the role of IKK α in the regulation of inflammasome activity, since loss of IKK α kinase activity is associated with spontaneous inflammatory diseases^{41, 42} and cancer^{43, 44}. Previously, Zhu et al reported on mice bearing a mutation in the ATP binding site of IKK α that resulted in loss of kinase activity (K44A)⁴⁵. Beginning at approximately 3 months of age, these mice developed severe skin lesions and systemic inflammation, with the eventual development of spontaneous squamous cell carcinoma (SCC) of the lung⁴². Additionally, mice expressing an inactivatable variant of IKK α (AA), in which the activating phosphorylation sites serines 176 and 180 were replaced with alanines, had increased susceptibility to bacterial- and LPS-induced shock⁴⁶. Moreover, loss of acinar cell IKK α triggers spontaneous pancreatitis in mice⁴¹.

In the present paper, we explore a novel mechanism by which IKK α regulates the inflammasome activation that might contribute to the inflammatory phenotypes in mice with loss of IKK α or its kinase activity. Loss of IKK α kinase activity results in markedly enhanced NLRP3, AIM2 and NLRC4 inflammasome activation, with aberrant caspase-1 activation and IL-1 β secretion. Furthermore, chimeric mice with loss of IKK α kinase activity in the hematopoietic compartment have significantly increased *in vivo* responses to the NLRP3 stimuli LPS and MSU, as well as greater inflammation in the acute silica-induced lung injury model. We show that IKK α controls the inflammasome at the level of the adaptor molecule ASC, which interacts with IKK α in the nucleus of resting macrophages in an IKK α kinase-dependent manner. IKKi (IKK-related kinase) facilitates the translocation of ASC from the nucleus to the perinuclear area during both NLRP3 (IRAK1/2-dependent) and AIM2 (IRAK1/2-independent) inflammasome activation. ASC remains under the control of IKK α in the perinuclear area following translocation of the ASC/IKK α complex. Signal 2 of NLRP3 activation leads to the inhibition of IKK α kinase activity through the recruitment of phosphatase PP2A, allowing dissociation of ASC from IKK α for participation in NLRP3 inflammasome assembly. Consistently, ASC is also released from IKK α during AIM2 and NLRC4 inflammasome activation. In summary, we identify a novel IKKi-IKK α -ASC axis that serves as a common regulatory mechanism to control ASC-containing inflammasomes.

Results

Loss of IKK α kinase activity leads to inflammasome hyperactivation

We first examined NLRP3 inflammasome activation in bone marrow-derived macrophages (BMDMs) from *IKK α K44A* mice and WT controls. Surprisingly, treatment with LPS alone was sufficient to cause cleavage of pro-caspase-1 in *IKK α K44A* BMDMs, whereas both LPS+ATP were needed for caspase-1 activation in WT BMDMs (Fig. 1a). Furthermore, combined treatment with LPS+ATP led to increased inflammasome activity in *IKK α K44A* BMDMs compared to that in control cells (Fig. 1a,b). Furthermore, ATP-induced inflammasome activation was significantly increased in *IKK α K44A* cells primed with alternative TLR ligands, including Pam₃CSK₄, R848, and CpG (Supplementary Fig. 1a).

Moreover, LPS alone was able to induce the interaction between ASC and pro-caspase-1 in *IKKα K44A* BMDMs, while in WT BMDMs the interaction was only detectable following treatment with both LPS+ATP (Fig. 1c). It is important to note that the increased inflammasome activity in *IKKα K44A* BMDMs was not due to higher basal levels of inflammasome proteins, as pro-caspase-1, ASC, NLRP3, and pro-IL-1β levels were comparable between *IKKα K44A* and WT cells (Fig. 1a). One consideration is the possible impact of IKKα on NFκB activation. Consistent with previous studies⁴⁷, NF-κB activation was actually comparable and even slightly decreased in *IKKα K44A* BMDMs, as indicated by IκBα phosphorylation and degradation (Supplementary Fig. 1b). Furthermore, we observed enhanced ATP-induced inflammasome activation following only 10 minutes of LPS priming in *IKKα K44A* BMDMs (Fig. 1d)^{21, 22, 24}. Additionally, *IKKα K44A* cells pre-treated with cyclohexamide showed significant caspase-1 activation following LPS stimulation alone, and greater caspase-1 activation than controls following LPS+ATP treatment, indicating that the enhanced inflammasome activation in *IKKα K44A* cells was not dependent on new protein synthesis (Supplementary Fig. 1c). Together, these findings strongly suggest that the inflammasome hyper-activation observed in IKKα K44A cells is due to a direct role of IKKα in inflammasome regulation. Consistently, *IKKα AA* BMDMs also showed enhanced inflammasome activation compared to controls (Fig. 1e).

Given the strong NLRP3 hyper-activation observed in cells with loss of IKKα kinase activity, we next sought to determine whether IKKα might also regulate other inflammasomes. *IKKα K44A* cells infected with the NLRC4 activator *S. typhimurium*²⁹ showed greatly enhanced caspase-1 activation (Fig. 1f). In addition, when *IKKα K44A* and *IKKα AA* BMDMs were transfected with the AIM2 ligand poly(dA:dT)^{28, 32, 34}, both IKKα mutants showed increased AIM2 activation (Fig. 1g). Together, these data suggested that IKKα serves a critical regulatory role for the NLRP3, NLRC4 and AIM2 inflammasomes.

IKKα negatively regulates the inflammasome *in vivo*

To characterize the *in vivo* consequence of the inflammasome hyperactivity that we observed in *IKKα K44A* BMDMs, we generated bone marrow chimeric mice with a wild-type background that received either WT or *IKKα K44A* bone marrow. While LPS alone is not sufficient to activate the inflammasome in wild-type macrophages *in vitro*, intra-peritoneal administration of LPS in mice leads to an NLRP3-dependent response^{7, 14, 27}. We found that following treatment with LPS, serum levels of IL-1β but not TNF-α were significantly higher in K44A→WT mice, and re-stimulation of K44A→WT splenocytes *in vitro* resulted in dramatically higher IL-1β production (Fig. 2a,b). Similarly, intra-peritoneal treatment of chimeric mice with monosodium urate (MSU) crystals resulted in increased neutrophil influx in K44A→WT mice, as well as higher serum levels of IL-1β (Fig. 2c). We next sought to verify these findings of *in vivo* NLRP3 hyperactivity using a silica-induced acute lung injury model. Using this model, both K44A→WT and control mice received intra-tracheal administration of sterilized silica dust. Thirty-six hours after silica exposure, bronchoalveolar lavage (BAL) fluid from K44A→WT mice contained significantly higher concentrations of IL-1β (Fig. 2e). In addition, histopathologic analysis of K44A→WT lungs revealed greater pulmonary inflammation than WT→WT lungs (Fig. 2d). In support of these

in vivo studies, inflammasome hyperactivation was also observed *ex vivo* in LPS-primed *IKKα K44A* macrophages in response to silica, MSU, and alum (Supplementary Fig 1d).

IKKα kinase activity is required for interaction with ASC

Since both *in vitro* and *in vivo* studies showed a profound loss of inflammasome regulation in the absence of IKKα kinase activity, we further investigated the interaction between IKKα and the inflammasome pathway. Co-immunoprecipitation studies in HEK293 cells co-transfected with ASC and either IKKα WT or IKKα K44A indicated that ASC interacts with IKKα WT but not IKKα K44A (Fig. 3a). Similarly, in primary BMDMs, ASC co-immunoprecipitated with endogenous IKKα WT, but failed to pull down IKKα K44A (Fig. 3b), indicating that IKKα constitutively interacts with ASC and the kinase activity of IKKα is required for this interaction. Importantly, we found that the IKKα-ASC interaction was nearly abolished upon treatment with LPS plus ATP (Fig. 3b,c and Supplementary Fig. 2a–c) or the bacterial pore-forming toxin gramicidin (Fig. 3c). Furthermore, pre-treatment with 5 mM glycine attenuated LPS plus ATP-induced cell death but not the dissociation of ASC from IKKα, indicating that the observed dissociation was not secondary to cytotoxicity (Supplementary Fig. 2a). LPS+ATP treatment was also able to induce the dissociation of ASC from IKKα in *caspase-1^{-/-}* macrophages (Supplementary Fig. 2b). Infection with *S. typhimurium* or transfection with poly(dA:dT) also led to the dissociation of ASC from IKKα (Fig. 3d), mirroring the results obtained with NLRP3 activators (Figs. 3b,c). In light of the constitutive interaction of IKKα with ASC, we reasoned that IKKα might be controlling ASC at the level of subcellular localization, which has been reported to be important for inflammasome regulation²³. In resting WT BMDMs, ASC was located almost exclusively in the nucleus, while in *IKKα K44A* BMDMs ASC was primarily located in the perinuclear area (Fig. 3e). Following stimulation of WT cells with LPS, ASC translocated to the perinuclear area, akin to what was observed in resting *IKKα K44A* cells (Fig. 3e). In marked contrast, stimulation of *IKKα K44A* cells with LPS resulted in the formation of ASC perinuclear specks (Fig. 3e). Importantly, the perinuclear ASC specks that formed in response to LPS treatment alone in *IKKα K44A* BMDMs co-stained with caspase-1 FLICA, indicating that these structures were participating in inflammasome assembly (Fig. 3e). The addition of LPS+ATP resulted in the formation of active ASC specks in both wild-type and *IKKα K44A* cells, while quantification revealed significantly more specks in *IKKα K44A* cells compared to controls (Fig. 3e). These findings suggest that IKKα regulates inflammasome activation at least in part by controlling the subcellular localization of ASC, and that in the absence of this regulation ASC is released to the perinuclear area, resulting in qualitative and quantitative inflammasome hyperactivity.

Interestingly, although LPS+ATP induced hyperactivation of the inflammasome in *IKKα AA* macrophages (Fig. 1e,g), ASC was actually located almost exclusively in the nucleus in resting *IKKα AA* cells (Fig. 3e). However, stimulation of *IKKα AA* cells with LPS alone also resulted in the formation of ASC perinuclear specks that co-stained with caspase-1 FLICA (Fig. 3e). Consistently ASC retained the interaction with IKKα AA at resting state, while the interaction was abolished upon LPS stimulation (Supplementary Fig. 2c). Furthermore, quantification revealed significantly more LPS+ATP-induced specks in *IKKα AA* cells

compared to wild-type cells (Fig. 3e). Taken together, these results support the critical role of IKK α in the regulation of inflammasome activation.

S193 and S16 of ASC are required for interaction with IKK α

In order to better understand the mechanism by which IKK α exerts control over, we screened the serine residues on ASC. We mutated 12 serine residues in ASC to alanine and co-expressed the mutants with IKK α in 293 cells. We identified two sites on ASC that when mutated have altered interaction with IKK α . While one site (S193A) showed a complete loss of interaction with IKK α , another site (S16A) had a moderate reduction in interaction with IKK α (Fig. 4a). We then immunoprecipitated wild-type ASC, S193A and S16A from 293 cells co-transfected with IKK α WT or IKK α K44A, followed by in vitro kinase assay. Co-expression of wild-type ASC with IKK α WT but not IKK α K44A resulted in phosphorylation of ASC (Fig. 4b). While S193A showed a complete loss of phosphorylation of ASC evident by the in vitro kinase assay, S16A had a moderate reduction in ASC phosphorylation (Fig. 4b). Since S193 is required for the interaction of ASC with IKK α , these results indicate that the interaction of ASC with kinase-active IKK α is important for ASC phosphorylation.

To examine the impact of S193A and S16A on inflammasome activation, we retrovirally infected ASC^{-/-} macrophages with wild-type ASC, S193A and S16A. Wild-type ASC interacted with endogenous IKK α , retained the interaction in the presence of LPS, and dissociated with IKK α upon stimulation with LPS+ATP (Fig. 4c). In contrast, S193A lost interaction with IKK α , while S16A retained interaction with endogenous IKK α , but dissociated with IKK α upon LPS stimulation (Fig. 4c). In ASC^{-/-} macrophages restored with wild-type ASC, ASC was located almost exclusively in the nucleus at resting state, whereas in S193A cells the majority of ASC was located in the perinuclear area (Fig. 4d). These results indicate that loss of interaction of S193A with IKK α released S193A from the nucleus, which is similar to the phenotype of ASC in IKK α K44A cells. Thus, S193 is a critical residue for the constitutive interaction of ASC with IKK α , which is required for the sequestration of ASC in the nucleus. In contrast, S16A only translocated to the perinuclear area in response to LPS stimulation, indicating that the interaction of S16A with IKK α was sufficient to retain S16A in the nucleus at resting state, mirroring the results from IKK α AA cells (Fig. 4d). However, stimulation of either S193A or S16A cells with LPS alone was sufficient for the formation of ASC perinuclear specks associated with inflammasome activation (Fig. 4d). Consistently, LPS alone was sufficient to cause cleavage of pro-caspase-1 in ASC^{-/-} macrophages infected with S193A and S16A, but not with wild-type ASC (Fig. 4e). Furthermore, treatment of S193A and S16A cells with LPS+ATP resulted in increased inflammasome activation compares to controls (Fig. 4e,4f). Thus, S16 is a critical residue required for the sustained interaction between IKK α -ASC after LPS-induced nuclear-cytoplasmic translocation, which is essential for IKK α -mediated ASC sequestration at the perinuclear area. Given that AIM2 inflammasome activation was also regulated by IKK α -mediated control of ASC (Fig. 3d), we extended this study by evaluating the impact of the S193A and S16A mutations on AIM2 activation. Transfection of S193A and S16A cells with poly(dA:dT) resulted in significantly enhanced AIM2 inflammasome activation (Fig. 4g).

ATP inhibits IKK α and releases ASC

LPS alone was able to activate the inflammasome in *IKK α K44A* and *IKK α AA* BMDMs (Fig. 3e), suggesting that ATP acts to remove the inhibitory effect of IKK α on ASC in wild-type cells. Given that IKK α dissociates from ASC upon LPS+ATP stimulation (Fig. 3b), we hypothesized that the second signal provided by ATP leads to the release of ASC from IKK α . Previous studies have shown that extracellular ATP requires the purinergic receptor P2X7R to induce inflammasome activation²⁶, and pre-treatment with the P2X7R antagonist AZ10606120 (AZ) indeed prevented pro-caspase-1 cleavage in response to LPS+ATP (Fig. 5a). Pre-treatment with AZ prevented the dissociation of IKK α from ASC upon treatment with LPS+ATP (Fig. 5a). Consistent with this, in *P2X7R^{-/-}* BMDMs, ASC retained interaction with IKK α after treatment with LPS+ATP (Fig. 5b). As a consequence, pro-caspase-1 cleavage was also abolished in *P2X7R^{-/-}* cells following treatment with LPS +ATP (Fig. 5c). Considering the fact that the IKK α K44A mutant failed to interact with ASC, the ATP/P2X7R-dependent dissociation of ASC from IKK α could be due to an impact on IKK α kinase activity. In support of this, BMDMs pre-treated with ATP had reduced phosphorylation of IKK α and I κ B α in response to LPS treatment (Fig. 5d). To confirm the inhibition of IKK α kinase activity by NLRP3 stimuli, we performed an *in vitro* kinase assay using IKK α immunoprecipitated from LPS stimulated BMDMs that were pre-treated with DMSO, ATP, or nigericin. In this assay, both ATP and nigericin dramatically attenuated LPS-induced I κ B α phosphorylation by IKK α (Fig. 5e). Furthermore, to determine whether ATP signaling was sufficient to inhibit the activity of activated IKK α , we performed *in vitro* kinase assay using LPS-primed macrophages treated with ATP. We found that the kinase activity of IKK α was still dramatically attenuated (Supplementary Fig. 3a). In addition, the inhibition of IKK α kinase activity by ATP was not secondary to caspase-1-dependent cell death, as pre-treatment with the caspase-1 inhibitor zYVAD did not prevent ATP-mediated IKK α inhibition (Supplementary Fig. 3b). Moreover, ATP-mediated IKK α inhibition was completely abolished in *P2X7R^{-/-}* BMDMs (Supplementary Fig. 3b). Taken together, these data indicate that the second signal provided by extracellular ATP attenuates IKK α kinase activity, thus releasing ASC from the inhibitory action of IKK α and allowing ASC to participate in inflammasome assembly.

We next sought to explore the mechanism by which ATP-P2X7R signaling inhibits IKK α kinase activity. It was previously reported that the serine/threonine phosphatase PP2A directly dephosphorylates IKK α , and that this event decreases I κ B α phosphorylation by IKK α ⁴⁸. In addition, others have reported that inhibition of PP2A and another closely related phosphatase, PP1, greatly diminished inflammasome activation in macrophages⁴⁹. We therefore speculated that PP2A might play a role in ATP-mediated IKK α inhibition. We found that PP2A indeed co-immunoprecipitated with IKK α following treatment with LPS +ATP, but not in resting cells or in response to LPS alone (Fig. 6a). Pre-treatment of BMDMs with the PP2A inhibitor okadaic acid and P2X7R inhibitor AZ prevented the interaction between IKK α and PP2A, and also abrogated the dissociation of ASC from IKK α (Fig. 6a). Pre-treatment with okadaic acid resulted in a dose-dependent decrease in inflammasome activation in response to LPS+ATP (Fig. 6b,c). In addition to ATP, the NLRP3 activator nigericin also induced interaction between PP2A and IKK α , while okadaic acid prevented this interaction (Fig. 6d) and led to a dose-dependent decrease in nigericin-

induced caspase-1 cleavage (Fig 6e). Furthermore, *PP2A* knockdown substantially attenuated caspase-1 activation (Fig. 6f). Importantly, the decreased NLRP3 inflammasome activity observed in response to okadaic acid and *PP2A* knockdown was not due to an indirect impact on LPS signaling, as TNF- α secretion was unaffected (Fig. 6c). Instead, we found that *PP2A* knockdown abolished ATP-mediated IKK α inhibition (Supplementary Fig. 3c) suggesting that *PP2A* plays a direct role in inhibiting IKK α in response to signal 2 of NLRP3 activation. We further found that blocking either K⁺ efflux or Ca²⁺ mobilization abolished the ATP- and nigericin-induced recruitment of *PP2A* to IKK α , suggesting that these cellular events, which are reported to be downstream of a multitude of NLRP3 activators^{50, 51}, may converge on *PP2A*-IKK α -ASC (Supplementary Fig. 3d). However, while *PP2A* activity was required for NLRP3 activation, *PP2A* knockdown had no effect on AIM2 inflammasome activation (Fig. 6g). Collectively, these data suggest that in LPS-primed macrophages, ATP and nigericin activate *PP2A* to inhibit IKK α , releasing ASC for participation in NLRP3 inflammasome formation.

IKKi facilitates ASC nuclear-to-cytoplasmic translocation

One important question is how LPS induces ASC-IKK α translocation. IRAK1 and IRAK2 are critical downstream mediators of the IL1-R/TLR pathway⁵²⁻⁵⁴, and a role for IRAK1 in acute NLRP3 inflammasome priming has recently been reported^{21, 24}. We found that inflammasome activation in response to treatment with LPS for 4 hours followed by ATP was completely abolished in *IRAK1/2*^{-/-} BMDMs (Supplementary Fig. 4a-c,e). *IRAK1/2* were also required for LPS-induced translocation of ASC-IKK α (Supplementary Fig. 5a). However, deficiency of *IRAK1/2* had no impact on perinuclear ASC speck formation in response to poly(dA:dT) (Supplementary Fig. 4d-e). We next asked what signaling molecule(s) might be acting downstream of *IRAK1/2* to promote NLRP3 inflammasome activation. Furthermore, given that *IRAK1/2* were actually dispensable for AIM2 inflammasome activation, we also hypothesized that there might be a common effector promoting ASC translocation during the activation of ASC-dependent inflammasomes. We focused on several of the kinases implicated in TLR4-IRAK1/2 downstream signaling, including TAK1⁵⁴, NIK⁵⁵, Mnk1/2⁵² and IKKi⁵⁶. Among the tested kinases (Supplementary Fig. 6a), we found that only IKKi deficiency resulted in dramatic reduction of inflammasome activation in response to LPS+ATP treatment, while having minimal impact on TNF- α secretion (Fig. 7a,b). We found that IKKi deficiency also resulted in decreased AIM2 activation (Fig. 7c). Consistently, IKKi deficiency resulted in greatly diminished ASC translocation in response to both LPS and poly(dA:dT), as well as decreased speck formation (Fig. 7d), suggesting that IKKi might be the common effector for ASC-dependent inflammasome activation.

S58 of ASC is a critical for IKKi-mediated ASC translocation

We further investigated how IKKi mediates inflammasome activation. Immunostaining showed that while IKKi was in the cytoplasm of untreated cells, LPS stimulation induced partial translocation of IKKi into the nucleus, some of which co-localized with ASC, while further treatment with ATP dispersed IKKi back to the cytoplasm (Fig. 7d). Co-immunoprecipitation experiments showed that LPS stimulation induced the interaction of IKKi with ASC, which was abolished upon ATP treatment (Fig. 7e). In addition, the LPS-

induced interaction between IKKi and ASC was completely abolished in *IRAK1/2*^{-/-} BMDMs (Supplementary Fig. 5b). Since IKKi interacted with ASC and co-localized with ASC in the nucleus in response to LPS stimulation, we hypothesized that IKKi might directly regulate ASC. To test the functional link between IKKi and ASC, ASC was co-expressed with wild-type IKKi or kinase dead IKKi (IKKi-KD). We found that co-expression of wild-type ASC with wild-type IKKi but not IKKi-KD resulted in phosphorylation of ASC (Fig. 8a), implying a functional role of IKKi in mediating ASC phosphorylation. In search of the residue(s) in ASC required for IKKi-mediated phosphorylation, we became interested in residue S58 of ASC due to the fact that the S58A mutant was reported to have substantially reduced inflammasome activation⁵⁷. We found that *ASC*^{-/-} macrophages restored with S58A showed abolished inflammasome activation in response to LPS+ATP stimulation (Supplementary Fig. 6b). Importantly, compared to wild-type ASC, S58A showed abolished phosphorylation when co-expressed with IKKi (Fig. 8a), indicating that residue S58 is required for IKKi-induced ASC phosphorylation.

Since IKKi is required for LPS-induced ASC nuclear-cytoplasmic translocation, we tested the S58A restored macrophages by confocal imaging. Similar to wild-type ASC, the S58A mutant was mostly retained in the nucleus of resting cells (Fig. 8b). While LPS induced translocation of wild-type ASC to the perinuclear area, S58A remained in the nucleus upon LPS stimulation (Fig. 8b). Furthermore, LPS+ATP-induced ASC speck formation was significantly reduced in S58A cells (Fig. 8b). Consistently, S58A remained in complex with IKK α even upon treatment with LPS+ATP (Fig. 8c). Moreover, AIM2 activation was also attenuated in S58A cells (Fig. 8b). Taken together, these results strongly suggest that S58 is a critical residue for ASC translocation to the perinuclear area, which might be achieved through IKKi-mediated phosphorylation of this residue.

Since S58A failed to translocate in response to LPS, we wondered whether this mutation would cause sequestration of S193A or S16A in the nucleus. Thus, we generated S193AS58A and S16AS58A double mutations and retrovirally introduced them into *ASC*^{-/-} macrophages, along with S193A and S16A. In these restored cells, LPS alone induced inflammasome activation in S193A, S16A and S193AS58A, whereas S16AS58A failed to promote inflammasome activation even when stimulated with LPS+ATP (Fig. 8d). Similar to S193A, S193AS58A was also perinuclear in resting cells and showed ASC speck formation in response to LPS, indicating that S58A mutation had no reversal effect on ASC S193A (Fig. 8e). Consistent with our findings from NLRP3 activation (Fig. 8d), we found that in S58A and S16AS58 cells, poly(dA:dT) resulted in dramatically decreased caspase-1 cleavage, while S193AS58A cells showed increased activation (Fig. 8f). Thus, the S58A mutation caused S16A sequestration in the nucleus, indicating that IKKi-mediated ASC phosphorylation through S58 is required for S16A translocation and consequent inflammasome activation.

Discussion

Although the inflammasomes play a central role in host defense and in many common human diseases, the regulatory mechanisms governing these important complexes have remained unclear. In this study, we identified IKK α as a critical negative regulator of ASC-

containing inflammasomes. IKK α constitutively interacts with the common inflammasome adaptor molecule ASC in a kinase activity-dependent manner, and loss of IKK α kinase activity results in hyperactivation of the NLRP3, AIM2, and NLRC4 inflammasomes. Mechanistically, the IKK-related kinase IKKi directly participates in NLRP3 inflammasome activation via LPS-induced interaction with ASC, driving the translocation and perinuclear re-organization of the ASC/IKK α complex. Following translocation of the ASC/IKK α complex, ASC remains under the control of IKK α in the perinuclear area. Signal 2 of NLRP3 activation leads to the inhibition of IKK α kinase activity through recruitment of PP2A, allowing dissociation of ASC from IKK α for participation in inflammasome assembly. Consistently, AIM2 and NLRC4 inflammasome activators also result in dissociation of ASC from IKK α . Together, these findings reveal a novel IKKi-IKK α -ASC axis that serves as a common regulatory mechanism to govern the ASC-dependent inflammasomes.

One question that arises from our study is the precise mechanism by which IKK α sequesters ASC in the nucleus of resting macrophages. In fact, it is possible that there is some degree of IKK α kinase activity in resting macrophages. It was previously reported that purified IKK α underwent autophosphorylation, whereas a kinase-inactive version of IKK α , in which the ATP binding site was mutated (K44M), showed no autophosphorylation⁵⁸. In the same report, it was shown that a related kinase, IKK β , although expressed in equivalent amounts, showed very weak autophosphorylation. We found that ASC is mainly located in the perinuclear area of resting *IKK α K44A* macrophages but is retained in the nucleus of *IKK α AA* cells, suggesting that IKK α might have basal activity that is independent of activating phosphorylation at S176/180, and that this activity is critical for the control of ASC. However, we cannot exclude the possibility that the differential impact of IKK α K44A versus IKK α AA on ASC localization in resting cells might also reflect structural differences. In addition to this IKK α -mediated regulation of ASC in the nucleus, we further found that IKK α continues to control ASC after LPS-induced perinuclear re-organization. It is interesting to note that although S16A was retained in the nucleus of resting cells, this mutation allowed LPS-induced NLRP3 inflammasome activation without ATP, which resembles the phenotype of ASC in *IKK α AA* cells. Both *IKK α AA* and S16A macrophages also exhibit hyperactivation of the AIM2 and NLRC4 inflammasomes, implying that IKK α -mediated ASC sequestration at the perinuclear area is part of the common regulatory mechanism for the control of ASC-dependent inflammasomes following ASC/IKK α translocation.

Most previous studies in the field have viewed priming of the NLRP3 inflammasome as a passive process that permits the generation of rate-limiting components, in particular NLRP3^{14–19}. Several recent studies have demonstrated that other critical events also take place during this phase^{20–24}. Our own studies suggest that “signal 1” of NLRP3 activation initiates a cascade of signaling events that results in the movement of ASC-IKK α from the nucleus. Indeed, it was recently reported that the TLR pathway molecule IRAK1 plays a crucial role in facilitating ASC nuclear-to-cytosolic translocation during NLRP3 priming²⁴. We found that while IRAK1/2 double deficiency completely abolished NLRP3 activation, it had minimum impact on LPS-induced NLRP3 and pro-caspase-1 expression

(Supplementary Fig. 4a–c), probably due to the fact that IRAK1/2-deficiency has little impact on TLR4-induced NF κ B activation⁵⁴.

Excitingly, we found that IKKi is critical for the nuclear-to-cytosolic translocation of ASC and for consequent NLRP3 inflammasome activation. We also discovered that IKKi is also important for AIM2 activation, suggesting that IKKi plays a unique role in mediating ASC translocation and perinuclear re-organization in response to diverse ligands (both TLR-dependent and –independent), thus critically facilitating the activation of ASC-containing inflammasomes. It will be important to investigate whether AIM2 engages IKKi directly, or via additional intermediate molecules. An additional question posed by the finding that IKKi plays a central role in inflammasome activation is how TNF- α , which has also been shown to prime the NLRP3 inflammasome, might participate in inflammasome activation in an IKKi-dependent manner. Interestingly, IKKi has a well-described role in the TNF- α pathway, with TNF- α activating IKKi/TBK1 through a TAK1-IKK α / β -dependent pathway^{59, 60}. Furthermore, this same pathway also induces IKKi upregulation via NF- κ B-mediated IKKi gene transcription⁶¹. Therefore, it is possible that IKKi also promotes TNF α -induced priming. Future investigation is warranted to delineate the precise role of IKKi in this pathway.

The functional impact of IKKi on ASC was further investigated through the structure-functional analysis of ASC. Interestingly, our data suggest that S58 might be a potential phosphorylation site for IKKi, since S58A showed abolished phosphorylation when co-expressed with IKKi. Therefore, it is possible that this phosphorylation alters the conformation of ASC, or is critical for the interaction of ASC with a chaperone protein that then directly facilitates ASC translocation. It is also important to note that Syk and Jnk have recently been shown to direct phosphorylation of ASC, and that this phosphorylation is required for NLRP3 activation⁵⁷. It is possible that Syk or Jnk might act on ASC after ASC-IKK α translocation to the perinuclear area. These are important questions that should be addressed in subsequent studies.

Another important question in inflammasome biology is how diverse “signal 2” stimuli converge to activate the NLRP3 inflammasome¹³. Many cellular events have been proposed as key mediators of NLRP3 activation. Recently, K⁺ efflux⁵¹ and Ca²⁺ mobilization⁵⁰ have also been shown to play crucial roles in response to many NLRP3 stimuli. Here, we demonstrated that the inhibition of IKK α and the subsequent dissociation of ASC from IKK α occurred in response to NLRP3 stimuli. In search of intermediate signaling molecules for “signal 2”-mediated IKK α inhibition, PP2A was a candidate because it was previously shown to directly inactivate IKK α ⁴⁸. We found that pharmacologic inhibition and knockdown of PP2A prevented ASC dissociation from IKK α , and attenuated inflammasome activation. We further found that blocking either K⁺ efflux or Ca²⁺ mobilization abolished ATP- and nigericin-induced recruitment of PP2A to IKK α , suggesting that these events converge on the PP2A-IKK α -ASC axis. Based on these findings, we propose that “signal 2”-induced recruitment of PP2A to the IKK α -ASC complex results in IKK α inhibition and consequent liberation of ASC from IKK α . This liberated form of ASC may experience a conformational change, which is permissive for assembly of the inflammasome. It is important to point out that ASC was also released from IKK α during AIM2 inflammasome

activation. However, it remains unclear what drives the dissociation of ASC from IKK α for AIM2 activation, since PP2A was dispensable for the activation of AIM2. It is possible that some other phosphatase may act on IKK α during AIM2 activation, such as the closely related phosphatase PP1. Another possibility is that an intermediary molecule may act during AIM2 activation to disrupt IKK α -mediated suppression of ASC without the requirement for IKK α dephosphorylation, for example by competing with ASC. These will be important questions for future investigation.

Materials and Methods

Reagents

Ultrapure LPS (tlrl-pelps), Pam₃CSK₄ (tlrl-pms) and MSU (tlrl-msu) were purchased from Invivogen. LPS (E coli serotype 0111:B4), poly(dA:dT) (P0883), poly(I:C) (P1530) and ATP (A2383) were purchased from Sigma. Imject alum (77161) was purchased from ThermoScientific. Anti-caspase-1 (p20) antibody was generated as previously described by L. Franchi and G. Nunez. Anti-ASC (N-15)-R, anti-IKK α (SC-7218), anti-IKK α (SC-7182), anti-IRAK1 (H273), anti-Caspase1 p10 (M20), Anti-NLRP3 (H-66), Anti-IKKi (A-11) antibodies and normal rabbit IgG (SC-2027), normal mouse IgG (SC-2025) were purchased from Santa Cruz Biotechnology, Inc. Anti-ASC antibody (AL177) was purchased from Adipogen. Anti-ASC antibody (2EI-7) was purchased from Milipore. Anti-IKK α (14A321) was purchased from Millipore. Antibodies against phosphorylated Anti-I κ B α (Ser-32/36), Anti-p-IKK α / β (Ser-176/180), Anti-I κ B α (4812), Anti-GFP (2956), Anti-PP2Ac (2259), Anti-IKKi (3416) and Mouse anti-rabbit conformation specific mAb (3678) were purchased from Cell Signaling. Anti-neutrophil antibody (NIMP-R14) and anti-IRAK2 (ab62419) antibody were purchased from Abcam. Anti-IL-1 β antibody (3ZD) was obtained from the Biological Resources Branch of the NIH. AZ10606120 (3323) and okadaic acid (1136) were purchased from Tocris. Silica (MIN-U-SIL 5) was a gift from US Silica. Antibodies for flow cytometry were purchased from eBiosciences: FITC-Gr-1 (RB6.8C5), PE-Cy7CD11b (M1/70), PCP-Ly6C (HK1.4), APC-F4/80 (BM8), and APC-Cy7-CD11c. Anti-Mouse (GAM) and Anti-Rabbit (GAR) secondary antibody were purchased from Thermo scientific. All antibodies were used at a dilution of 1:1000 unless otherwise specified.

Mice

6–12 week old age- and gender-matched *IKK α K44A*⁴², *IKK α AA*⁴⁶, *P2X7R*^{-/-25}, *IRAK1*^{-/-54}, *IRAK2*^{-/-54}, *Caspase-1*^{-/-62}, *IKKi*^{-/-63}, and *NIK*^{-/-64} mice were previously described. All studies were performed according to National Institutes of Health guidelines and were approved by the Institutional Animal Care and Use Committee of the Cleveland Clinic, Case Western Reserve University, and the National Cancer Institute. For in vivo experiments, we performed a power analysis based on our previous experience with each technique, including effect size and variation within and between experiments. Mice were numbered and then treated and sacrificed according to a randomized protocol.

Generation of bone marrow chimeric mice

6–10 week old **age- and gender-matched** WT recipient mice were gamma-irradiated with 950 rad using the ¹³⁷Cs irradiator facility at the Frederick National Laboratory. Recipient mice were then injected *i.v.* with 1×10^6 WT or *IKKa K44A* BM cells isolated from 10-week old female mice. Single cell suspensions of BM cells were prepared by passing dissociated long bone cells through a 40 μ m strainer followed by washing with PBS.

LPS shock and peritonitis induction

Mice were injected intra-peritoneally with either 30 mg/kg Ultrapure LPS (Invivogen) or 100 mg MSU (Invivogen) resuspended in a total volume of 100 μ l endotoxin-free PBS. Serum was collected 2 hours post-LPS treatment and 5 hours-post MSU treatment. Peritoneal lavage was carried out at the same as serum collection, and used 5 mL total volume PBS. Total lavage volume was spun and cells were counted and stained surface stained for Gr-1, CD11b, Ly6c, F4/80, and CD11c for flow cytometric analysis.

Silica-induced lung inflammation

Mice were anesthetized using a combination of ketamine (80 mg/kg) and xylazine (10 mg/kg). Silica-induced lung injury was then induced by instillation of 1 mg sterilized silica particles in 100 μ l of sterile saline as previously described⁶⁵. BAL fluid was collected from anesthetized mice using a 0.8 ml PBS wash of the lungs (5 times) with a 22-gauge catheter.

Cell Preparation

Unless otherwise indicated, all cells were cultured at 37° C. Bone marrow-derived macrophages (BMDMs) were obtained from bone marrow of tibia and femur and cultured by DMEM with 20% FBS and 30% L929 cell-conditioned medium and penicillin/streptomycin for differentiation and proliferation of BMDMs. Cells were differentiated for 5 days, and then re-plated and used for experiments the following day. 293T cells were purchased from ATCC (Manassas, VA). Immortalized WT and *ASC^{-/-}* BMDMs were previously described¹⁰.

Retroviral production and restoration of immortalized macrophages

For infection of immortalized macrophages, viral supernatants were collected 36 hours after transfection of Phoenix cells with 5 μ g empty vector, mASC WT, mASC S193A, mASC S16A, mASC S58A, mASC S58AS193A and mASC S58AS16A, which had all been cloned into pMx-IP vector. After 48 hours of infection, puromycin (10 μ g/ml) was added to the cells to select for restored cells. Mouse ASC mutant constructs were designed using the following primer pairs: ASC S16A forward-GGACGCTCTTGAAAACCTGG CAGGGGATGAAC, ASC S16A reverse-GTTCATCCCCTGCCAAGTTTTCAAGAGCGTCC; ASC S193A forward-GTGATGGACCTGGAGCAGGCCTGAGAATTCAAGC, ASC S193A reverse-GCTTGAATTCTCAGGCCTGCTCCAGGTCCATCAC; ASC S58A forward-CAAACCTGTGCCTACTATCTGGAGTCGTATGGCTTGG; ASC S58A reverse-CCAAGCCATACGACTCCAGATAGTAGGCGACAAGTTTG.

Inflammasome activation

BMDMs were plated in 6-well plates at a concentration of 2.0×10^6 cells per well the day before the experiment. The day of the experiment, cells were primed with LPS (1 $\mu\text{g}/\text{ml}$), Pam₃CSK₄ (1 $\mu\text{g}/\text{ml}$), R848 (1 $\mu\text{g}/\text{ml}$), or CpG-B (1 $\mu\text{g}/\text{ml}$) for the indicated time. Medium was then supplemented with ATP (5 mM) for indicated timepoints. For AIM2 inflammasome activation, cells were transfected with 1.5 $\mu\text{g}/\text{ml}$ poly(dA:dT) using lipofectamine 2000 transfection reagent in OPTI-MEM media. For NLRC4 inflammasome activation, *Salmonella typhimurium* (SL 1344) was added at an MOI of 50, and after 30 minutes gentamycin was added to the medium. For all experiments, cell-free supernatant was then either collected for ELISA analysis, or cell lysates and supernatants were collected together for immunoblotting by the addition of 1% Nonidet-P40 supplemented with complete protease inhibitor 'cocktail' (Roche) and 2 mM dithiothreitol directly to the well. Cells were scraped and lysed on ice for 30 minutes, then spun at 13,000 rpm. Protein concentration was measured. 4X Laemmli buffer was then added, samples were boiled and approximately 20 μg of sample was run on a 12% or 15% SDS-PAGE gel.

Immunoprecipitation and pull-down assay

BMDMs were plated in a 15 cm dish 1–2 days before the experiment at a concentration of 1×10^6 cells per ml. The day of the experiment, cells were stimulated as indicated. After washing with cold PBS, cells were lysed in 0.5 ml of lysis buffer (50 mM Tris-HCL, pH 7.4, 150 mM NaCl, 1% Triton, 1 mM EDTA, 5 mM NaF, 2 mM NaVO₃, 1 mM PMSF, 1 \times complete protease inhibitors). Cell lysates were cleared by centrifugation at 13,000 rpm for 10 min, and insoluble debris was discarded. Then supernatants were precleared by incubation with agarose beads for 1 h at 4 °C followed by centrifugation at 3000 rpm. For co-immunoprecipitations, precleared supernatants were incubated with 20 μl of protein A-Sepharose beads with antibody at 4 °C overnight, and beads were washed with 1 ml of lysis buffer 5 times before dissolved in 40 μl of Laemmli buffer.

Immunoblotting

Whole cell lysates and or immunoprecipitates were dissolved in Laemmli buffer and resolved by 10%–15% SDS-PAGE. After electrophoresis, separated proteins were transferred onto polyvinylidene difluoride membrane (Millipore). For immunoblotting, the polyvinylidene difluoride membrane was blocked with 5% nonfat milk. After incubation with specific primary antibody, horseradish peroxidase-conjugated secondary antibody was applied. The positive immune reactive signal was detected by ECL (Amersham Biosciences).

Confocal Analysis

BMDMs were treated as indicated. Cells were then fixed in 4% paraformaldehyde for 10–15 min, washed, and blocked with Signal Enhancer. Cells were reacted with anti-ASC, anti-IKKi and caspase-1 FLICA (FAM-YVAD-FMK), washed, and incubated with Alexa-488 (green) or Alexa-555 (red) secondary antibody.

Biochemical assays

Mouse IL-1 β and TNF- α in cell culture supernatants were measured using IL-1 β and TNF- α Duo-Set kits purchased from R&D systems, and were used according to the manufacturer's instructions. LDH was measured using the Cytotox 96 Non-Radioactive Cytotoxicity Assay (Promega).

In vitro kinase assays

Cells were washed twice with ice-cold PBS, and lysed using Co-IP buffer for 30 min on ice. Cell lysate (600 μ l) was immunoprecipitated with indicated antibody in the presence of protein A-agarose beads overnight at 4°C with constant agitation. The beads were washed twice with Co-IP buffer following by two additional washes with kinase buffer (20 mM HEPES, pH 7.5, 10 mM MgCl₂, 25 mM NaCl, 20 mM β -glycerophosphate, and 10 mM sodium orthovanadate). Washed beads were incubated with 30 μ l kinase buffer including 50 μ M of cold ATP, 5 μ Ci of radioactive ATP (γ -³²P ATP) and with/without indicated substrate at 30°C for 30 min. The reaction was stopped by the addition of 4x sample buffer and heating for 5 min at 95°C. Proteins were subjected to SDS-PAGE, followed by autoradiography.

Statistics

Non-parametric statistical analysis was applied to all data sets. The *P* values of for all comparisons were determined by Mann-Whitney test unless otherwise noted. *P*<0.05 was considered to be significant. Unless otherwise specified, all center values represent the mean while error bars represent the s.e.m.

Supplementary Material

Refer to Web version on PubMed Central for supplementary material.

Acknowledgments

We gratefully acknowledge Shao-Cong Sun (University of Texas MD Anderson Cancer Center) and Rong-fu Wang (Methodist Hospital) for generously providing *NIK*^{-/-} and *TAK1*^{-/-} bones, respectively. We also thank members of the Li and DUBYAK laboratories for providing technical expertise and reagents. This work was supported by NIH grants P01HL029582-26A1, P01CA062220-16A1, and 1R01NS071996-01A1 to X.L.

References

1. Latz E. The inflammasomes: mechanisms of activation and function. *Current opinion in immunology*. 2010; 22:28–33. [PubMed: 20060699]
2. Rathinam VA, Vanaja SK, Fitzgerald KA. Regulation of inflammasome signaling. *Nature immunology*. 2012; 13:333–332. [PubMed: 22430786]
3. Strowig T, Henao-Mejia J, Elinav E, Flavell R. Inflammasomes in health and disease. *Nature*. 2012; 481:278–286. [PubMed: 22258606]
4. Vajjhala PR, Mirams RE, Hill JM. Multiple binding sites on the pyrin domain of ASC protein allow self-association and interaction with NLRP3 protein. *The Journal of biological chemistry*. 2012; 287:41732–41743. [PubMed: 23066025]
5. Bae JY, Park HH. Crystal structure of NALP3 protein pyrin domain (PYD) and its implications in inflammasome assembly. *The Journal of biological chemistry*. 2011; 286:39528–39536. [PubMed: 21880711]

6. Srinivasula SM, et al. The PYRIN-CARD protein ASC is an activating adaptor for caspase-1. *The Journal of biological chemistry*. 2002; 277:21119–21122. [PubMed: 11967258]
7. Mariathasan S, et al. Cryopyrin activates the inflammasome in response to toxins and ATP. *Nature*. 2006; 440:228–232. [PubMed: 16407890]
8. Kanneganti TD, et al. Critical role for Cryopyrin/Nalp3 in activation of caspase-1 in response to viral infection and double-stranded RNA. *The Journal of biological chemistry*. 2006; 281:36560–36568. [PubMed: 17008311]
9. Martinon F, Petrilli V, Mayor A, Tardivel A, Tschopp J. Gout-associated uric acid crystals activate the NALP3 inflammasome. *Nature*. 2006; 440:237–241. [PubMed: 16407889]
10. Hornung V, et al. Silica crystals and aluminum salts activate the NALP3 inflammasome through phagosomal destabilization. *Nature immunology*. 2008; 9:847–856. [PubMed: 18604214]
11. Dostert C, et al. Innate immune activation through Nalp3 inflammasome sensing of asbestos and silica. *Science*. 2008; 320:674–677. [PubMed: 18403674]
12. Franchi L, Eigenbrod T, Nunez G. Cutting edge: TNF-alpha mediates sensitization to ATP and silica via the NLRP3 inflammasome in the absence of microbial stimulation. *J Immunol*. 2009; 183:792–796. [PubMed: 19542372]
13. Latz E, Xiao TS, Stutz A. Activation and regulation of the inflammasomes. *Nature reviews. Immunology*. 2013; 13:397–411.
14. He Y, Franchi L, Nunez G. TLR agonists stimulate Nlrp3-dependent IL-1beta production independently of the purinergic P2X7 receptor in dendritic cells and in vivo. *J Immunol*. 2013; 190:334–339. [PubMed: 23225887]
15. Kahlenberg JM, Lundberg KC, Kertesz SB, Qu Y, Dubyak GR. Potentiation of caspase-1 activation by the P2X7 receptor is dependent on TLR signals and requires NF-kappaB-driven protein synthesis. *J Immunol*. 2005; 175:7611–7622. [PubMed: 16301671]
16. Bauernfeind F, et al. NLRP3 inflammasome activity is negatively controlled by miR-223. *J Immunol*. 2012; 189:4175–4181. [PubMed: 22984082]
17. Bauernfeind FG, et al. Cutting edge: NF-kappaB activating pattern recognition and cytokine receptors license NLRP3 inflammasome activation by regulating NLRP3 expression. *J Immunol*. 2009; 183:787–791. [PubMed: 19570822]
18. Embry CA, Franchi L, Nunez G, Mitchell TC. Mechanism of impaired NLRP3 inflammasome priming by monophosphoryl lipid A. *Science signaling*. 2011; 4:ra28. [PubMed: 21540455]
19. Bauernfeind F, et al. Cutting edge: reactive oxygen species inhibitors block priming, but not activation, of the NLRP3 inflammasome. *J Immunol*. 2011; 187:613–617. [PubMed: 21677136]
20. Py BF, Kim MS, Vakifahmetoglu-Norberg H, Yuan J. Deubiquitination of NLRP3 by BRCC3 critically regulates inflammasome activity. *Molecular cell*. 2013; 49:331–338. [PubMed: 23246432]
21. Fernandes-Alnemri T, et al. Cutting edge: TLR signaling licenses IRAK1 for rapid activation of the NLRP3 inflammasome. *J Immunol*. 2013; 191:3995–3999. [PubMed: 24043892]
22. Juliana C, et al. Non-transcriptional priming and deubiquitination regulate NLRP3 inflammasome activation. *The Journal of biological chemistry*. 2012; 287:36617–36622. [PubMed: 22948162]
23. Bryan NB, Dorfleutner A, Rojanasakul Y, Stehlik C. Activation of inflammasomes requires intracellular redistribution of the apoptotic speck-like protein containing a caspase recruitment domain. *J Immunol*. 2009; 182:3173–3182. [PubMed: 19234215]
24. Lin KM, et al. IRAK-1 bypasses priming and directly links TLRs to rapid NLRP3 inflammasome activation. *Proceedings of the National Academy of Sciences of the United States of America*. 2014; 111:775–780. [PubMed: 24379360]
25. Qu Y, et al. Pannexin-1 is required for ATP release during apoptosis but not for inflammasome activation. *J Immunol*. 2011; 186:6553–6561. [PubMed: 21508259]
26. Solle M, et al. Altered cytokine production in mice lacking P2X(7) receptors. *The Journal of biological chemistry*. 2001; 276:125–132. [PubMed: 11016935]
27. Sutterwala FS, et al. Critical role for NALP3/CIAS1/Cryopyrin in innate and adaptive immunity through its regulation of caspase-1. *Immunity*. 2006; 24:317–327. [PubMed: 16546100]

28. Hornung V, et al. AIM2 recognizes cytosolic dsDNA and forms a caspase-1-activating inflammasome with ASC. *Nature*. 2009; 458:514–518. [PubMed: 19158675]
29. Mariathasan S, et al. Differential activation of the inflammasome by caspase-1 adaptors ASC and Ipaf. *Nature*. 2004; 430:213–218. [PubMed: 15190255]
30. Franchi L, et al. NLR4-driven production of IL-1beta discriminates between pathogenic and commensal bacteria and promotes host intestinal defense. *Nature immunology*. 2012; 13:449–456. [PubMed: 22484733]
31. Kanneganti TD, et al. Bacterial RNA and small antiviral compounds activate caspase-1 through cryopyrin/Nalp3. *Nature*. 2006; 440:233–236. [PubMed: 16407888]
32. Rathinam VA, et al. The AIM2 inflammasome is essential for host defense against cytosolic bacteria and DNA viruses. *Nature immunology*. 2010; 11:395–402. [PubMed: 20351692]
33. Ichinohe T, Pang IK, Iwasaki A. Influenza virus activates inflammasomes via its intracellular M2 ion channel. *Nature immunology*. 2010; 11:404–410. [PubMed: 20383149]
34. Fernandes-Alnemri T, Yu JW, Datta P, Wu J, Alnemri ES. AIM2 activates the inflammasome and cell death in response to cytoplasmic DNA. *Nature*. 2009; 458:509–513. [PubMed: 19158676]
35. Sutterwala FS, et al. Immune recognition of *Pseudomonas aeruginosa* mediated by the IPAF/NLR4 inflammasome. *The Journal of experimental medicine*. 2007; 204:3235–3245. [PubMed: 18070936]
36. Hoffman HM, Mueller JL, Broide DH, Wanderer AA, Kolodner RD. Mutation of a new gene encoding a putative pyrin-like protein causes familial cold autoinflammatory syndrome and Muckle-Wells syndrome. *Nature genetics*. 2001; 29:301–305. [PubMed: 11687797]
37. Heneka MT, et al. NLRP3 is activated in Alzheimer's disease and contributes to pathology in APP/PS1 mice. *Nature*. 2013; 493:674–678. [PubMed: 23254930]
38. Henao-Mejia J, et al. Inflammasome-mediated dysbiosis regulates progression of NAFLD and obesity. *Nature*. 2012; 482:179–185. [PubMed: 22297845]
39. Duewell P, et al. NLRP3 inflammasomes are required for atherogenesis and activated by cholesterol crystals. *Nature*. 2010; 464:1357–1361. [PubMed: 20428172]
40. Vandanmagsar B, et al. The NLRP3 inflammasome instigates obesity-induced inflammation and insulin resistance. *Nature medicine*. 2011; 17:179–188.
41. Li N, et al. Loss of acinar cell IKKalpha triggers spontaneous pancreatitis in mice. *The Journal of clinical investigation*. 2013; 123:2231–2243. [PubMed: 23563314]
42. Xiao Z, et al. The pivotal role of IKKalpha in the development of spontaneous lung squamous cell carcinomas. *Cancer cell*. 2013; 23:527–540. [PubMed: 23597566]
43. Park E, et al. Reduction in IkappaB kinase alpha expression promotes the development of skin papillomas and carcinomas. *Cancer research*. 2007; 67:9158–9168. [PubMed: 17909021]
44. Liu B, et al. A critical role for I kappaB kinase alpha in the development of human and mouse squamous cell carcinomas. *Proceedings of the National Academy of Sciences of the United States of America*. 2006; 103:17202–17207. [PubMed: 17079494]
45. Zhu F, et al. IKKalpha shields 14-3-3sigma, a G(2)/M cell cycle checkpoint gene, from hypermethylation, preventing its silencing. *Molecular cell*. 2007; 27:214–227. [PubMed: 17643371]
46. Lawrence T, Bebien M, Liu GY, Nizet V, Karin M. IKKalpha limits macrophage NF-kappaB activation and contributes to the resolution of inflammation. *Nature*. 2005; 434:1138–1143. [PubMed: 15858576]
47. Hu Y, et al. Abnormal morphogenesis but intact IKK activation in mice lacking the IKKalpha subunit of IkappaB kinase. *Science*. 1999; 284:316–320. [PubMed: 10195896]
48. DiDonato JA, Hayakawa M, Rothwarf DM, Zandi E, Karin M. A cytokine-responsive IkappaB kinase that activates the transcription factor NF-kappaB. *Nature*. 1997; 388:548–554. [PubMed: 9252186]
49. Luheshi NM, Giles JA, Lopez-Castejon G, Brough D. Sphingosine regulates the NLRP3-inflammasome and IL-1beta release from macrophages. *European journal of immunology*. 2012; 42:716–725. [PubMed: 22105559]

50. Murakami T, et al. Critical role for calcium mobilization in activation of the NLRP3 inflammasome. *Proceedings of the National Academy of Sciences of the United States of America*. 2012; 109:11282–11287. [PubMed: 22733741]
51. Munoz-Planillo R, et al. K(+) efflux is the common trigger of NLRP3 inflammasome activation by bacterial toxins and particulate matter. *Immunity*. 2013; 38:1142–1153. [PubMed: 23809161]
52. Wan Y, et al. Interleukin-1 receptor-associated kinase 2 is critical for lipopolysaccharide-mediated post-transcriptional control. *The Journal of biological chemistry*. 2009; 284:10367–10375. [PubMed: 19224918]
53. Wan Y, et al. The dual functions of IL-1 receptor-associated kinase 2 in TLR9-mediated IFN and proinflammatory cytokine production. *J Immunol*. 2011; 186:3006–3014. [PubMed: 21270393]
54. Zhou H, et al. IRAK-M mediates Toll-like receptor/IL-1R-induced NF-kappaB activation and cytokine production. *The EMBO journal*. 2013; 32:583–596. [PubMed: 23376919]
55. Senftleben U, et al. Activation by IKKalpha of a second, evolutionary conserved, NF-kappa B signaling pathway. *Science*. 2001; 293:1495–1499. [PubMed: 11520989]
56. Hemmi H, et al. The roles of two IkappaB kinase-related kinases in lipopolysaccharide and double stranded RNA signaling and viral infection. *The Journal of experimental medicine*. 2004; 199:1641–1650. [PubMed: 15210742]
57. Hara H, et al. Phosphorylation of the adaptor ASC acts as a molecular switch that controls the formation of speck-like aggregates and inflammasome activity. *Nature immunology*. 2013; 14:1247–1255. [PubMed: 24185614]
58. Mercurio F, et al. IKK-1 and IKK-2: cytokine-activated IkappaB kinases essential for NF-kappaB activation. *Science*. 1997; 278:860–866. [PubMed: 9346484]
59. Clark K, et al. Novel cross-talk within the IKK family controls innate immunity. *The Biochemical journal*. 2011; 434:93–104. [PubMed: 21138416]
60. Kravchenko VV, Mathison JC, Schwamborn K, Mercurio F, Ulevitch RJ. IKKi/IKKepsilon plays a key role in integrating signals induced by pro-inflammatory stimuli. *The Journal of biological chemistry*. 2003; 278:26612–26619. [PubMed: 12736252]
61. Wang N, Ahmed S, Haqqi TM. Genomic structure and functional characterization of the promoter region of human IkappaB kinase-related kinase IKKi/IKKvarepsilon gene. *Gene*. 2005; 353:118–133. [PubMed: 15939554]
62. Karmakar M, Sun Y, Hise AG, Rietsch A, Pearlman E. Cutting edge: IL-1beta processing during *Pseudomonas aeruginosa* infection is mediated by neutrophil serine proteases and is independent of NLRP4 and caspase-1. *J Immunol*. 2012; 189:4231–4235. [PubMed: 23024281]
63. Tenover BR, et al. Multiple functions of the IKK-related kinase IKKepsilon in interferon-mediated antiviral immunity. *Science*. 2007; 315:1274–1278. [PubMed: 17332413]
64. Yin L, et al. Defective lymphotoxin-beta receptor-induced NF-kappaB transcriptional activity in NIK-deficient mice. *Science*. 2001; 291:2162–2165. [PubMed: 11251123]
65. Sato T, et al. Heme oxygenase-1, a potential biomarker of chronic silicosis, attenuates silica-induced lung injury. *American journal of respiratory and critical care medicine*. 2006; 174:906–914. [PubMed: 16858012]

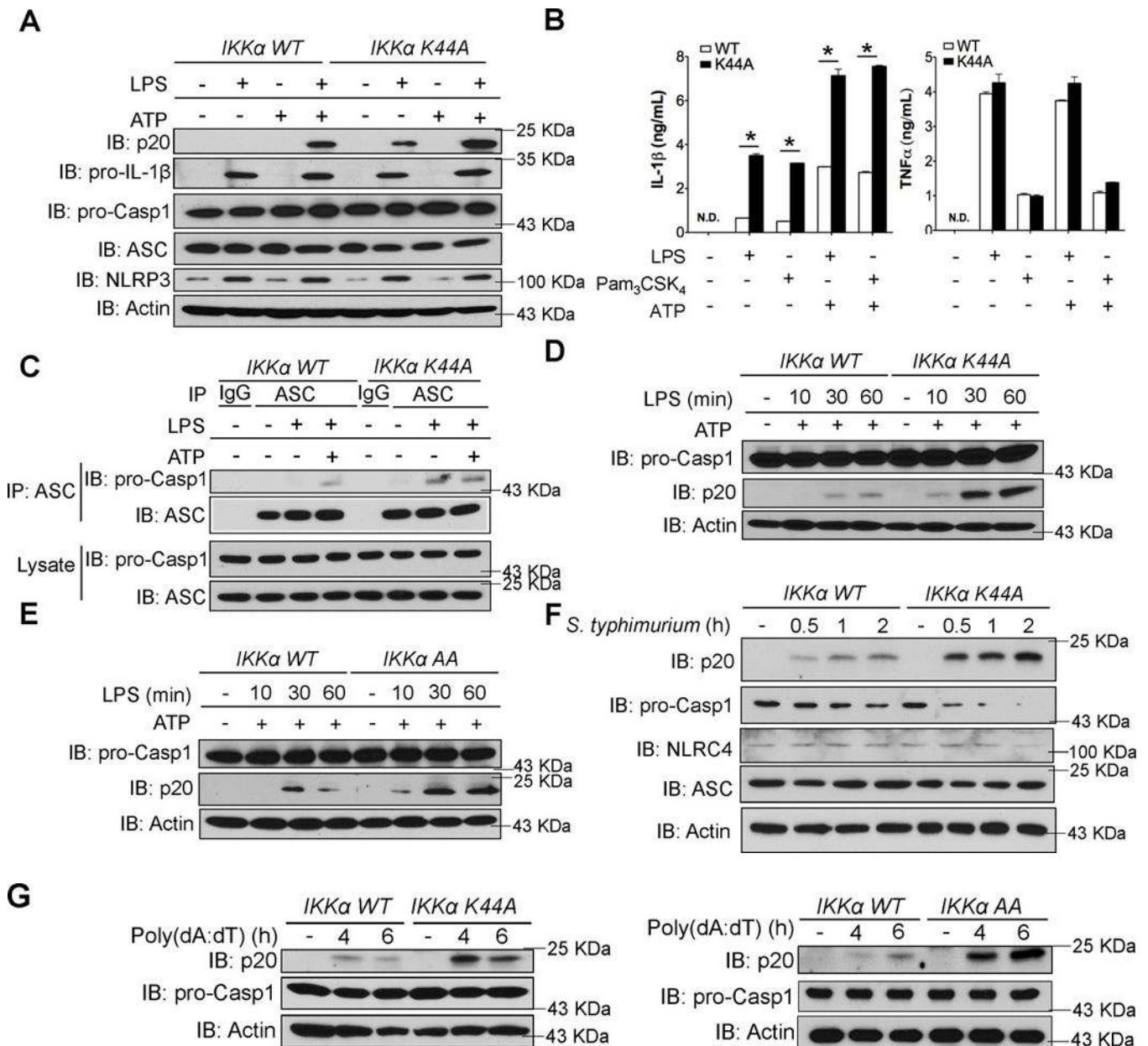


Figure 1. IKKα is a negative regulator of the inflammasome (a) BMDMs from WT and *IKKα* K44A mice were either left untreated or treated with LPS (1 μg/ml) for 4 hours, 5 mM ATP (30 min), or LPS (1 μg/ml) 4 hours + 5 mM ATP (30 min). Cell lysates and supernatants were collected together and were immunoblotted with the indicated antibodies. (b) Cell-free supernatants were collected from BMDMs that were either left untreated, or treated with LPS (1 μg/ml) for 4 hours, Pam₃CSK₄ (1 μg/ml) for 4 hours, LPS (1 μg/ml) 4 hours + 5 mM ATP (30 min), or Pam₃CSK₄ (1 μg/ml) 4 hours + 5 mM ATP (30 min). Levels of IL-1β and TNF-α were measured by ELISA. (c) BMDMs from WT and *IKKα* K44A mice were left untreated or treated with LPS (1 μg/ml) for 4 hours, or LPS (1 μg/ml) 4 hours + 5 mM ATP (30 min). Cell lysates were collected and immunoprecipitated with anti-ASC antibody or

control IgG antibody, followed by immunoblotting with the indicated antibodies. **(d,e)** BMDMs from WT and either *IKK α K44A* (**d**) or *IKK α AA* (**e**) mice were treated with LPS (1 $\mu\text{g}/\text{mL}$) for 0, 10, 30, or 60 minutes, followed by the addition of 5 mM ATP for 30 minutes. **(f)** BMDMs from WT and *IKK α K44A* mice were infected with *Salmonella typhimurium* at a multiplicity of infection (MOI) of 50 for 0, 0.5, 1, or 2 hours. Cell lysates and supernatants were then collected together and immunoblotted with the indicated antibodies. **(g)** BMDMs from WT, *IKK α K44A* (**left panel**) and *IKK α AA* mice (**right panel**) were transfected with poly(dA:dT) (1.5 $\mu\text{g}/\text{ml}$) using lipofectamine 2000. After indicated times, cell lysates and supernatants were collected together and immunoblotted with the indicated antibodies. N.D. indicates not detectable, and “UN” indicates left untreated. Data are representative of at least five independent experiments. Error bars represent s.e.m. of technical replicates. * $P < 0.05$ by Mann-Whitney test.

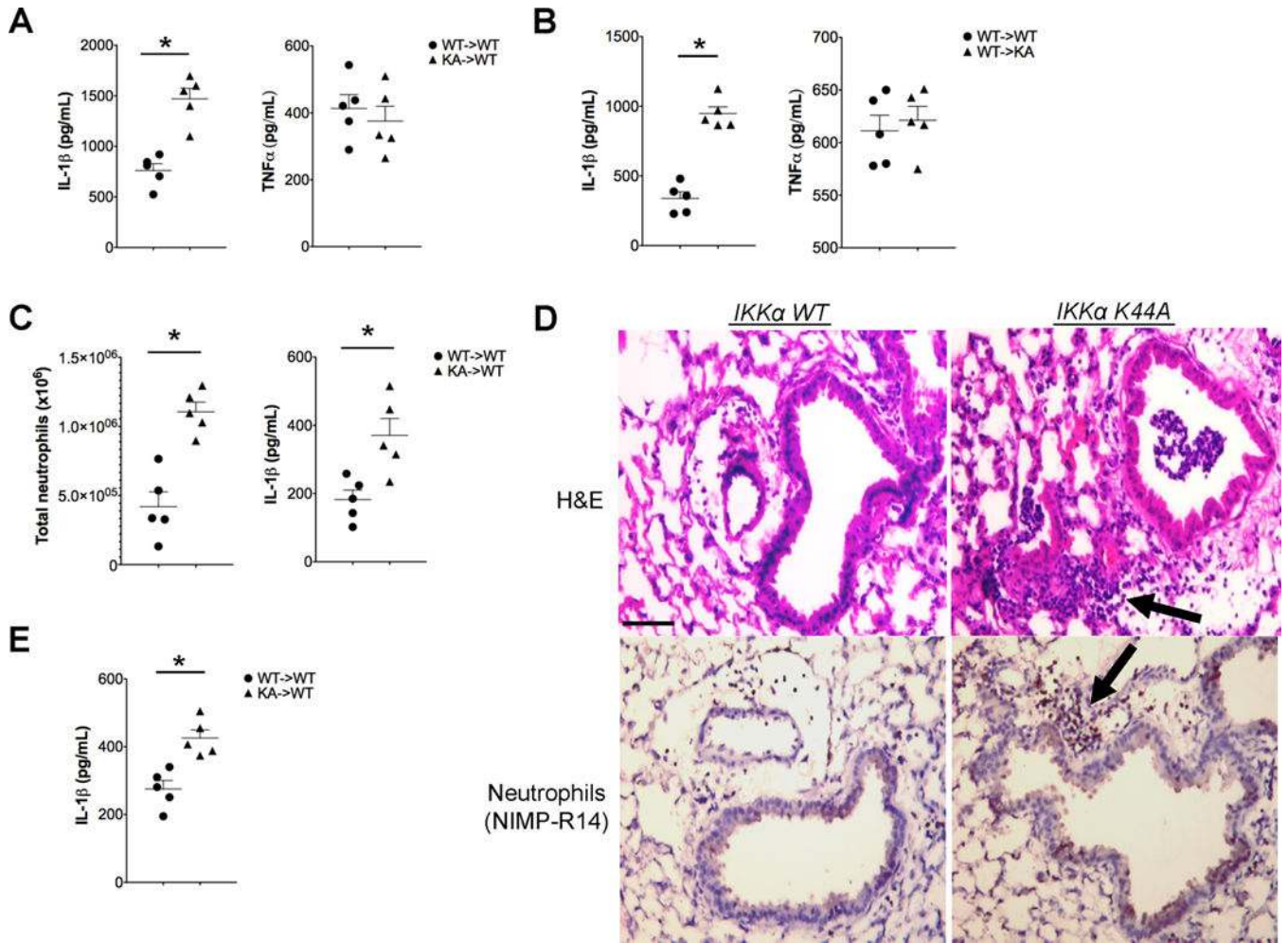
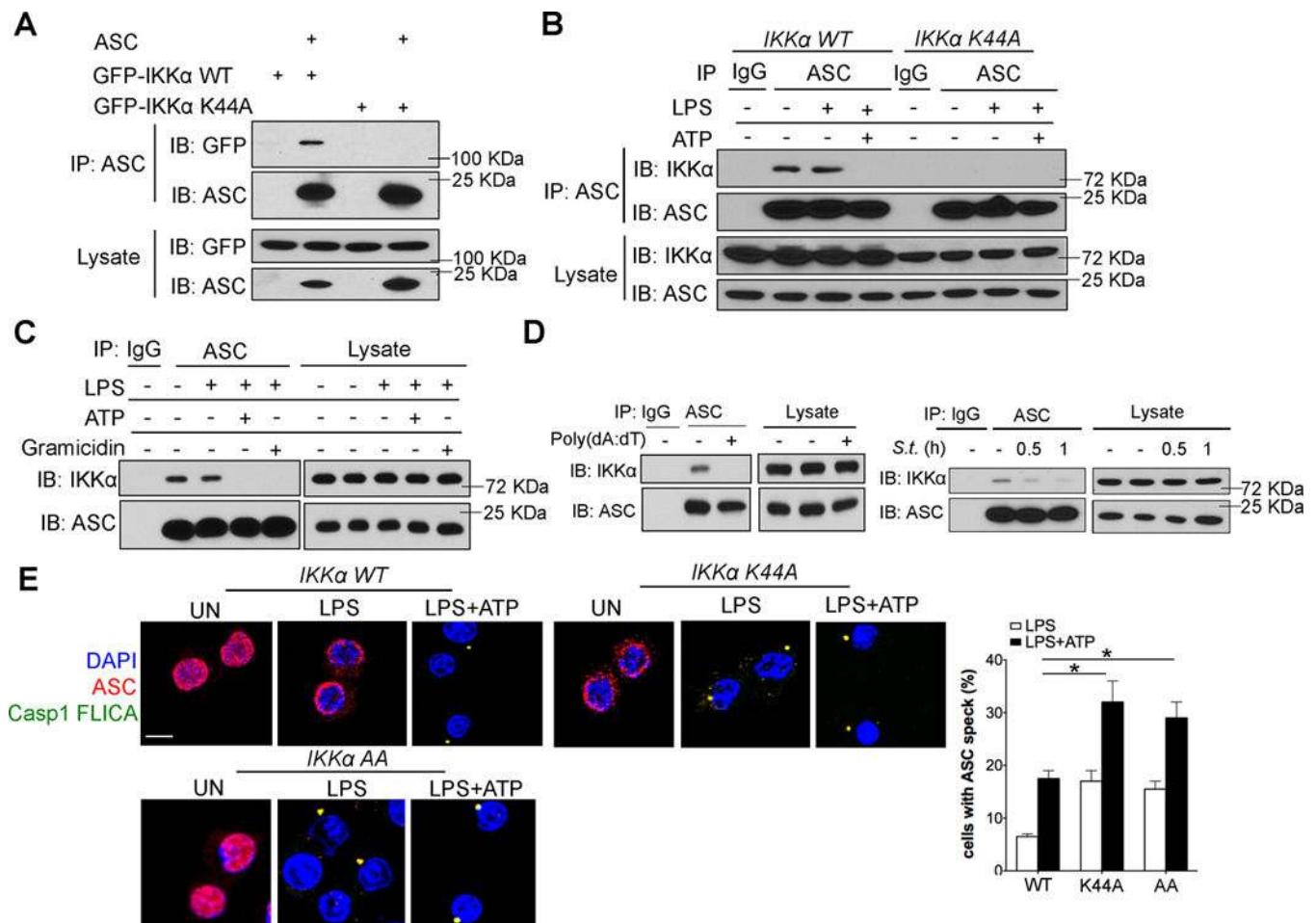


Figure 2. IKK α is a critical regulator of NLRP3 inflammasome activation *in vivo* (a,b) Irradiated WT mice received bone marrow from either WT or IKK α K44A mice. After six weeks of engraftment, chimeric mice received 30 mg/kg Ultrapure LPS in 100 μ l PBS (i.p). Serum was collected after 2 hours and levels of IL-1 β and TNF- α were measured by ELISA (a). Splenocytes were collected and cultured for 2 hours with or without re-stimulation with LPS (1 μ g/ml). Cell-free supernatants were collected and levels of IL-1 β and TNF- α were measured by ELISA (b). (c) Chimeric mice as described in (a) received 1 mg MSU in 100 μ l PBS (i.p). Five hours later, peritoneal lavage was performed and infiltrating neutrophils were quantified (left panel). Serum was collected and IL-1 β levels were determined by ELISA (right panel). (d,e) Chimeric mice as described in (a) received 1 mg sterilized silica by intra-tracheal instillation. Thirty-six hours later, lungs were harvested and lung sections were stained with hematoxylin and eosin (upper panels) or with anti-neutrophil antibody (NIMP-R14) (lower panels); scale bar represents 50 μ m (d). Broncho-alveolar lavage (BAL) was performed and IL-1 β levels in cell-free BAL fluid was assessed by ELISA (e). N.D. indicates not detectable, and “UN” indicates left untreated. Data are representative of two independent experiments. $n = 5$ mice per group in each experiment. Error bars represent s.e.m. of biological replicates. * $P < 0.05$ by Mann-Whitney test.

**Figure 3.**

IKK α regulates the inflammasome via interaction with ASC (a) HEK 293 cells were transfected with ASC and either GFP- IKK α WT or GFP-IKK α K44A using lipofectamine 2000. Empty vector was used to normalize total plasmid transfected. Cells were then lysed, followed by immunoprecipitation with anti-ASC antibody and immunoblotting with the indicated antibodies. (b,c) BMDMs from WT and *IKK α K44A* mice (b) or WT mice only (c) were either left untreated or treated with LPS (1 μ g/ml) for 4 hours, or LPS (1 μ g/ml) 4 hours + 5 mM ATP (30 min) (b), or either left untreated or treated with LPS (1 μ g/ml) for 4 hours, LPS (1 μ g/ml) 4 hours + 5 mM ATP (30 min), or LPS (1 μ g/ml) 4 hours + 1 μ M gramicidin (30 min) (c). Cell lysates were then immunoprecipitated using anti-ASC antibody or control IgG antibody, and were immunoblotted with the indicated antibodies. (d) BMDMs from WT mice were transfected with poly(dA:dT) (1.5 μ g/ml) using lipofectamine 2000 for 4 hours (left panel), or were infected with 50 MOI of *S. typhimurium* for indicated times (right panel). Cell lysates were then immunoprecipitated using anti-ASC antibody or control IgG antibody, and were immunoblotted with the indicated antibodies. (e) WT, *IKK α K44A* and *IKK α AA* BMDMs were either left untreated or treated with LPS (1 μ g/ml) for 4 hours, or LPS (1 μ g/ml) 4 hours + 5 mM ATP (30 min), then washed, fixed, and stained with anti-ASC antibody and caspase-1 FLICA (FAM-YVAD-FMK). Images were then acquired using confocal microscopy with a 60X objective

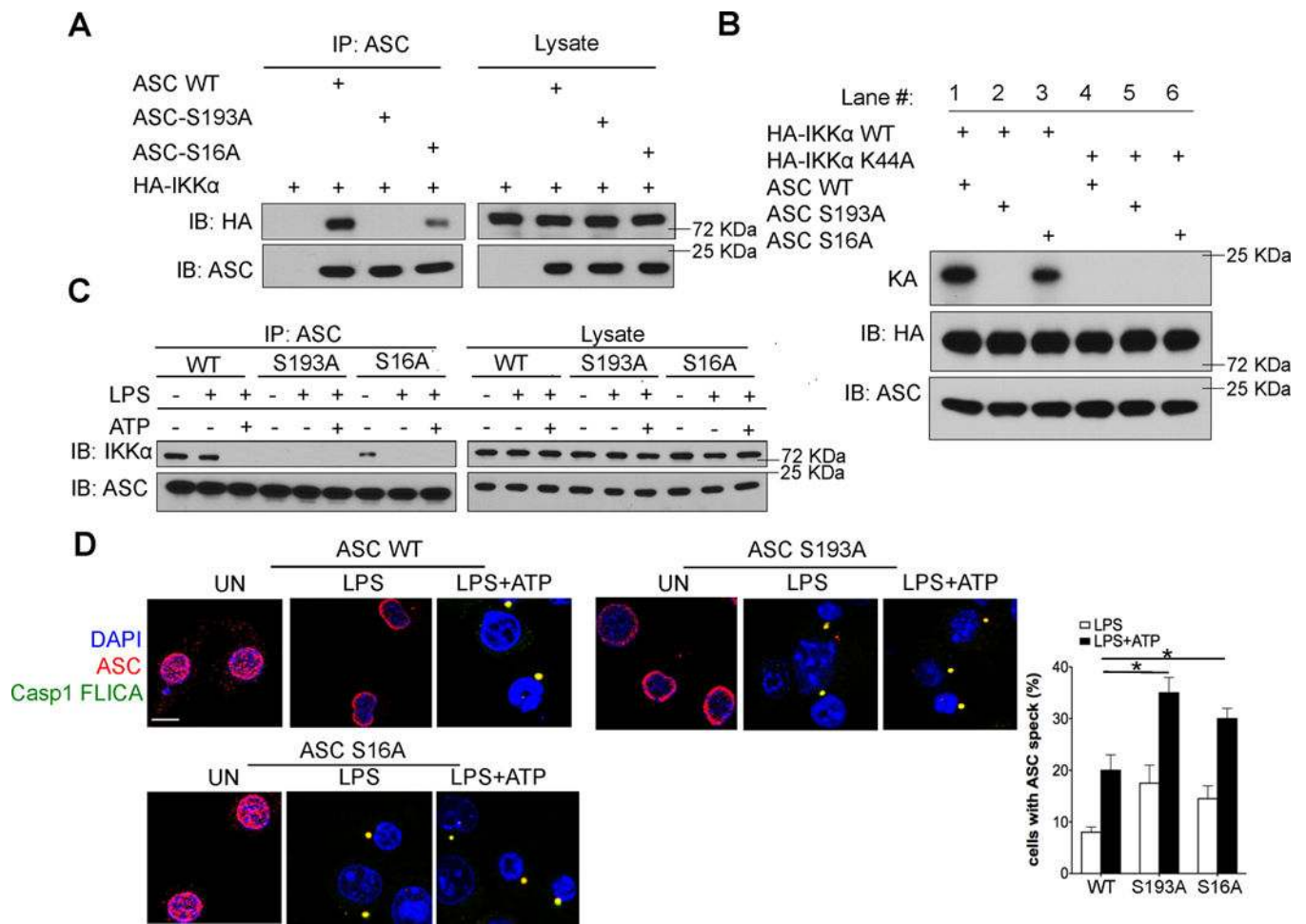
and 4X enlargement; scale bars are 5 μm . Images were quantified by counting number of cells with ASC specks co-staining with caspase-1 FLICA as a percentage of total cells counted in three fields. (**far right panel**). “UN” indicates left untreated. Data are representative of at least four independent experiments. Error bars represent s.e.m. of technical replicates. * $P < 0.05$ by Mann-Whitney test.

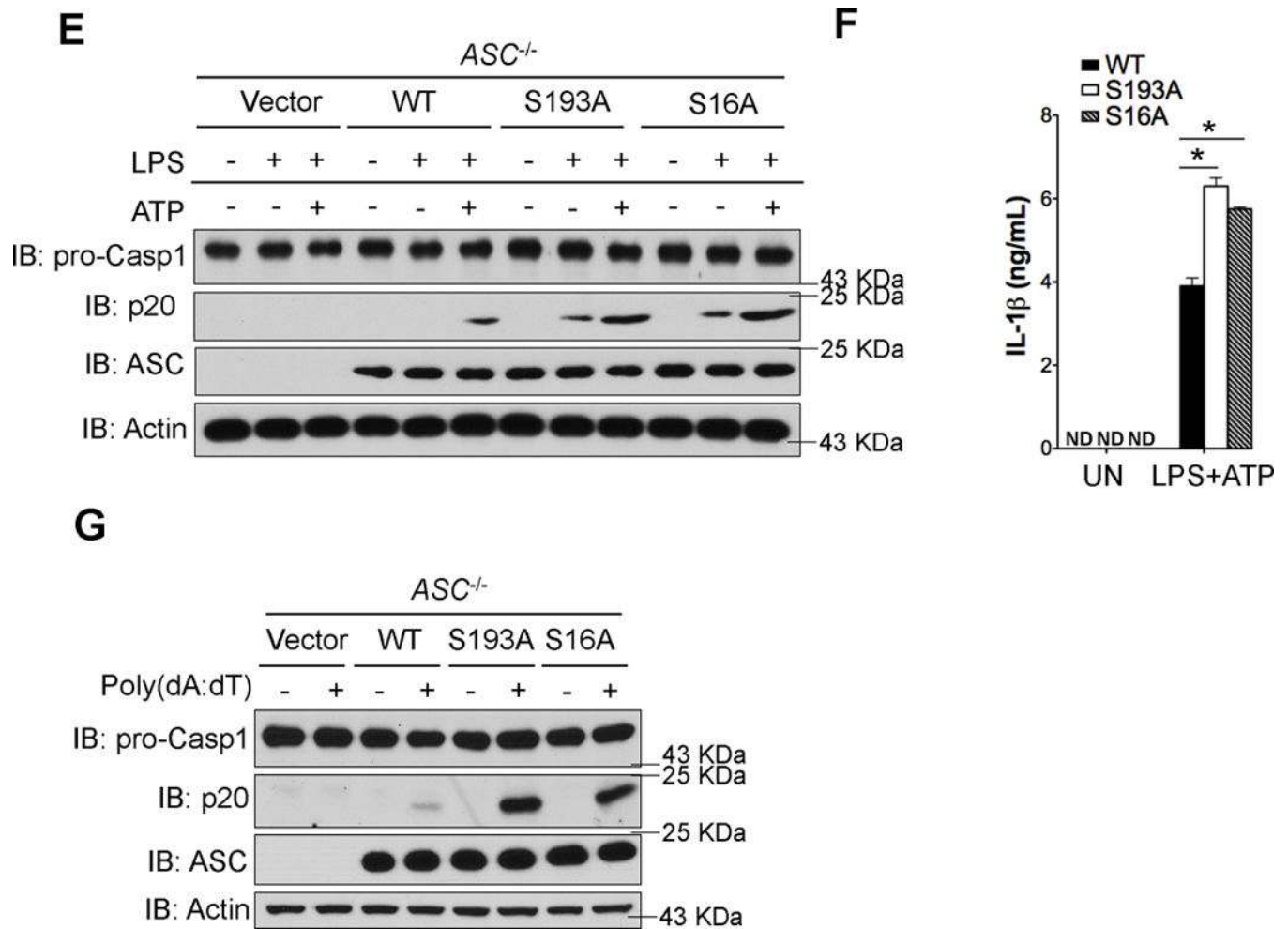
Author Manuscript

Author Manuscript

Author Manuscript

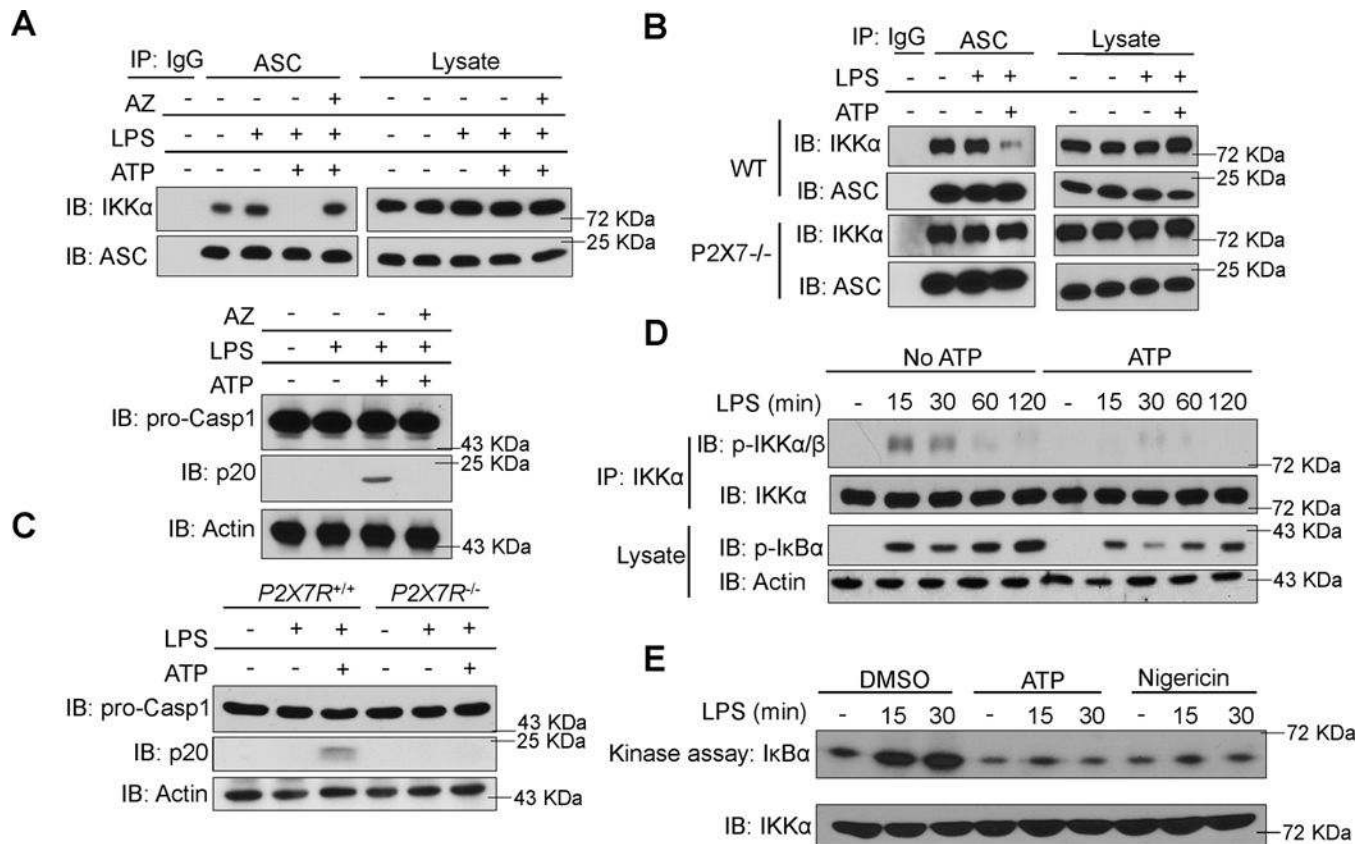
Author Manuscript



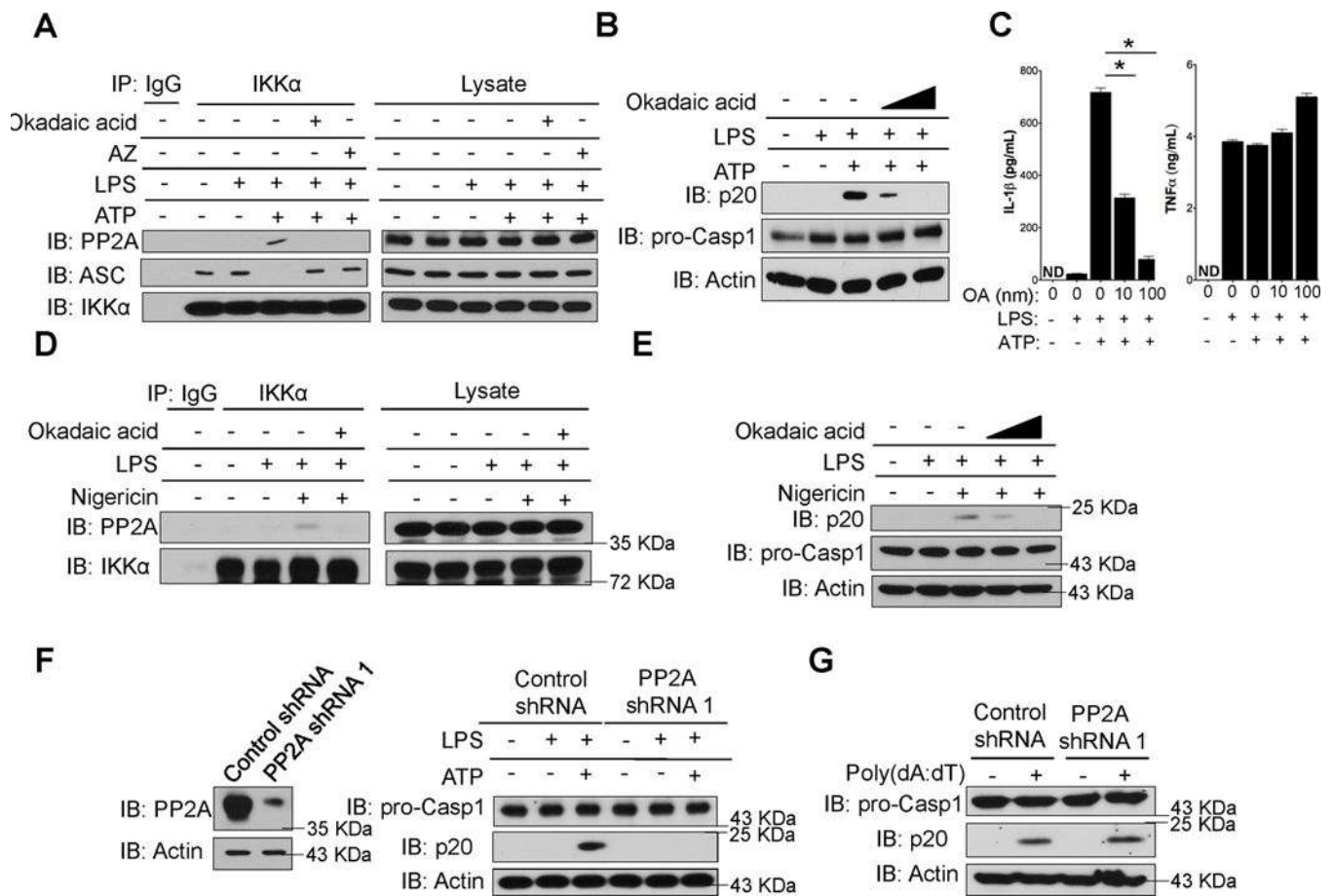
**Figure 4.**

S193 and S16 are critical residues on ASC for interaction with IKK α (a) HEK 293 cells were transfected with HA-IKK α and either WT ASC, S16A ASC, or S193A ASC using lipofectamine 2000. Empty vector was used to normalize total plasmid transfected. Cells were then lysed, followed by immunoprecipitation with anti-ASC antibody and immunoblotting with the indicated antibodies. (b) HEK 293 cells were transfected with HA-IKK α or HA-IKK α K44A along with either WT ASC, S16A ASC, or S193A ASC using lipofectamine 2000. Empty vector was used to normalize total plasmid transfected. Cells were then lysed, followed by immunoprecipitation with anti-ASC antibody and in vitro kinase assay. (c,d) Immortalized ASC^{-/-} macrophages retrovirally reconstituted with empty vector, WT ASC, S193A ASC, or S16A ASC were either left untreated or treated with LPS (1 μ g/mL) for 4 hours, followed by 30 min 5 mM ATP when indicated. Cells were then lysed, followed by immunoprecipitation with anti-ASC antibody and immunoblotting with indicated antibodies (c), or cells were then washed, fixed, and stained with anti-ASC antibody and caspase-1 FLICA (FAM-YVAD-FMK). Images were then acquired using confocal microscopy with 60X magnification and 4X enlargement; scale bars are 5 μ m (d). Images from were quantified by counting the number of cells with ASC specks co-staining with caspase-1 FLICA as a percentage of total cells counted in three fields. (e-g)

Retrovirally reconstituted $ASC^{-/-}$ macrophages from (c) were either left untreated or treated with LPS (1 $\mu\text{g}/\text{ml}$) for 4 hours, followed by 30 minutes of 5 mM ATP when indicated (e,f), or were transfected with poly(dA:dT) (1.5 $\mu\text{g}/\text{ml}$) using lipofectamine 2000 for 4 hours (g). Cell lysates and supernatants were then collected together and immunoblotted with the indicated antibodies (e,g), or were analyzed by ELISA (f). N.D. indicates not detectable, and “UN” indicates left untreated. Data are representative of at least four independent experiments. Error bars represent s.e.m. of technical replicates. * $P < 0.05$ by Mann-Whitney test.

**Figure 5.**

ATP signaling through P2X7R inhibits IKK α and releases ASC (a) BMDMs from WT mice were pre-treated with either DMSO or the P2X7R antagonist AZ10606120 (AZ) at a concentration of 10 nM for 30 min. Cells were then left untreated or treated with LPS (1 μ g/ml) for 4 hours, or LPS (1 μ g/ml) 4 hours + 5 mM ATP (30 min). Cell lysates were immunoprecipitated with anti-ASC antibody or control IgG antibody, and immunoblotted with the indicated antibodies (*upper panel*). Some cell lysates that were not used for immunoprecipitation were immunoblotted with other antibodies as indicated (*lower panel*). (b,c) BMDMs from WT and P2X7R^{-/-} mice were either left untreated or treated with LPS (1 μ g/ml) for 4 hours, or LPS (1 μ g/ml) 4 hours plus 5 mM ATP (30 min). Cell lysates were immunoprecipitated with anti-ASC antibody or control IgG antibody, and were then immunoblotted with the indicated antibodies (b). Cell lysates not used for immunoprecipitation were immunoblotted with the indicated antibodies (c). (d) BMDMs from WT mice were pre-treated with 5 mM ATP 15 minutes prior to treatment with LPS (1 μ g/ml) for 0, 15, 30, 60, or 120 minutes. Cells were then lysed and immunoprecipitated with anti-IKK α antibody. Immunoprecipitated proteins were eluted and immunoblotted for p-IKK α / β and IKK α . Lysates obtained before immunoprecipitated were immunoblotted for p-I κ B α and Actin. (e) WT BMDMs were pre-treated with 5 mM ATP or 10 μ M nigericin for 5 minutes, then treated with LPS (1 μ g/ml) for 0, 15, or 30 minutes. Cells were then lysed and immunoprecipitated with anti-IKK α antibody, followed by in vitro kinase assay using GST-I κ B α (1–317) as substrate. Data are representative of at least four independent experiments. Error bars represent s.e.m. of technical replicates. * $P < 0.05$ by Mann-Whitney test.

**Figure 6.**

PP2A activity is required for NLRP3 inflammasome activation (**a,d**) BMDMs from WT mice were pre-treated with DMSO, 100 nM okadaic acid (OA), or 10 nM AZ10606120 for 15 minutes. Cells were then left untreated or treated with LPS (1 μ g/ml) for 4 hours, LPS (1 μ g/ml) 4 hours plus 5 mM ATP (30 min), LPS (1 μ g/ml) 4 hours plus 5 mM ATP (30 min) plus OA (100nM) or LPS (1 μ g/ml) 4 hours plus 5 mM ATP (30 min) plus AZ10606120 (10 nM) (a) or 10 uM nigericin (30 min) (d). Cell lysates were immunoprecipitated using anti-IKK α antibody, and immunoblotted with the indicated antibodies. (**b,c,e**) BMDMs from WT mice were pre-treated with either DMSO or 10 nM or 100 nM okadaic acid for 15 minutes. Cells were then left untreated or treated with LPS (1 μ g/ml) for 4 hours, or LPS (1 μ g/ml) 4 hours + 5 mM ATP (30 min) (b, c) or 10 uM nigericin (30 min) (e). Cell lysates and supernatants were collected together and were immunoblotted with the indicated antibodies (b,e), and cell-free supernatants were collected and IL-1 β and TNF- α levels were assessed by ELISA (c). (**f,g**) WT BMDMs were infected with lentivirus containing either control or anti-PP2A-C shRNA. Cells were either left untreated or treated with LPS (1 μ g/ml) for 4 hours, followed by 5 mM ATP for 30 min when indicated (**f**), or were transfected with poly(dA:dT) (1.5 μ g/ml) using lipofectamine 2000 for 4 hours (**g**). After the indicated time, cell lysates and supernatants were collected together and immunoblotted with indicated antibodies. N.D. indicates not detectable, and "UN" indicates left untreated. Data are

representative of at least four independent experiments. Error bars represent s.e.m. of technical replicates. * $P < 0.05$ by Mann-Whitney test.

Author Manuscript

Author Manuscript

Author Manuscript

Author Manuscript

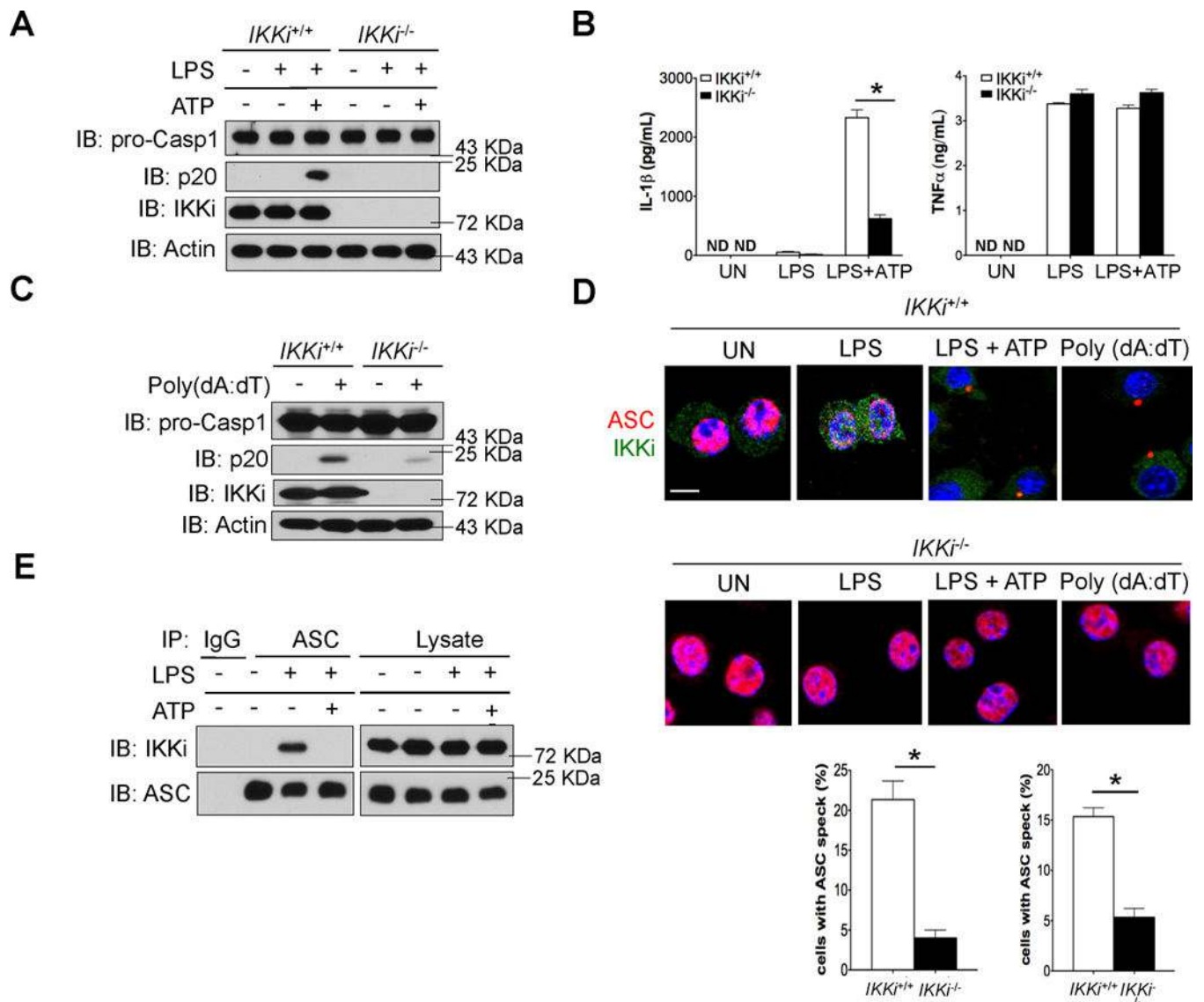
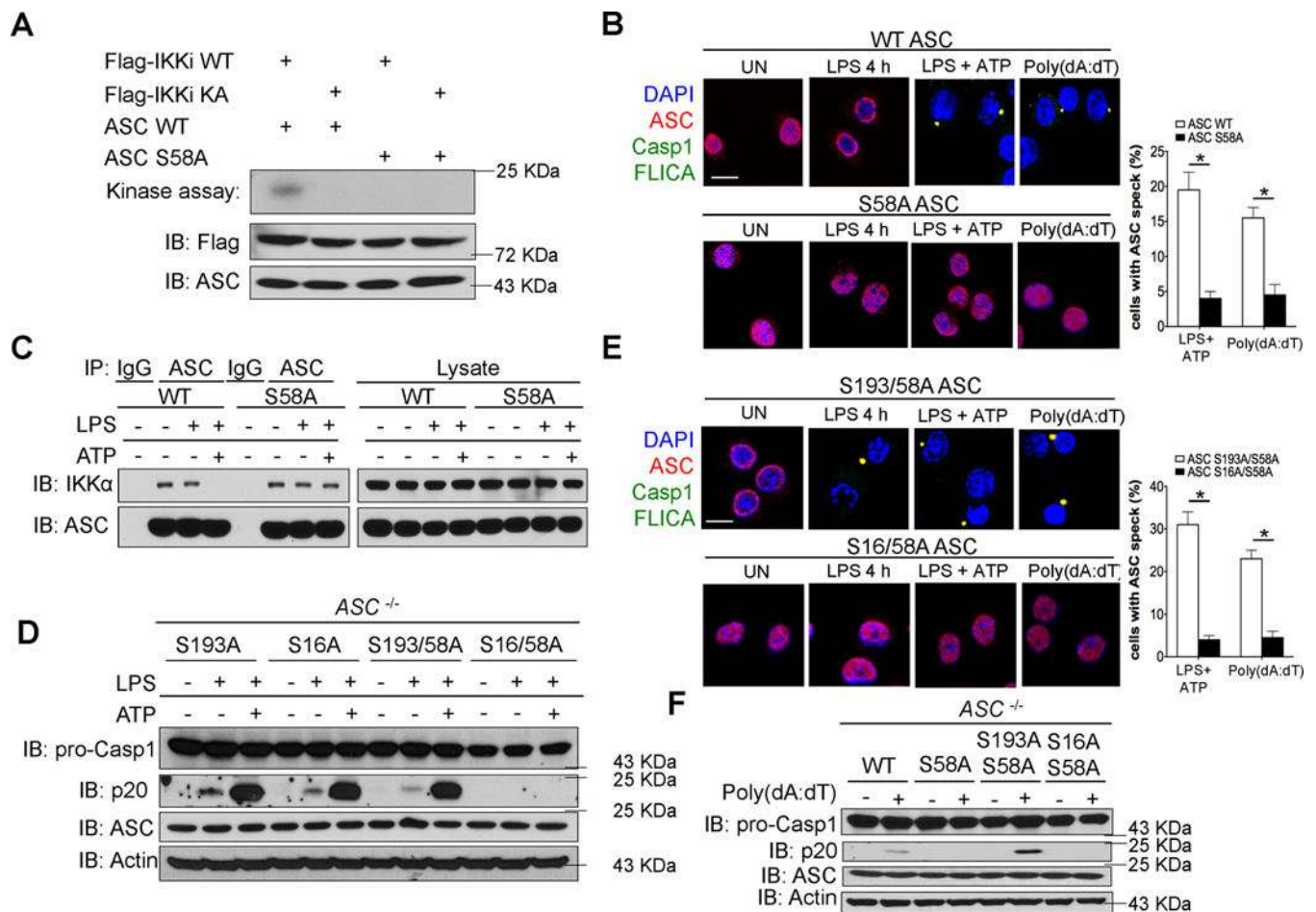


Figure 7. IKK α is required for ASC nuclear-to-cytosolic translocation and inflammasome activation (a) BMDMs from WT and *IKK α ^{-/-}* mice were treated with LPS (1 μ g/ml) for 4 hours, followed by 30 min 5 mM ATP when indicated. Cell lysates and supernatants were then collected together and immunoblotted with the indicated antibodies. (b) Cell-free supernatants from (a) were analyzed by ELISA to determine levels of IL-1 β (left panel) and TNF- α (right panel). (c) BMDMs from WT and *IKK α ^{-/-}* mice were transfected with poly(dA:dT) (1.5 μ g/ml) using lipofectamine 2000 for 4 hours. Cell lysates and supernatants were then collected together and immunoblotted with the indicated antibodies. (d) BMDMs from WT and *IKK α ^{-/-}* mice were left untreated or treated with LPS (1 μ g/ml) for 4 hours, LPS 4 hours + 5 mM ATP (30 min), or were transfected with poly(dA:dT) (1.5 μ g/ml) using lipofectamine 2000 for 4 hours. Cells were then washed and fixed, and stained with anti-ASC antibody and anti-IKK α antibody. Images were acquired using confocal microscopy with 60X magnification and 4X enlargement; scale bars are 5 μ m (upper panels). LPS

+ATP- and poly(dA:dT)-treated samples were quantified by counting the number of cells with ASC specks as a percentage of total cells counted in three fields. **(lower panels) (e)** BMDMs from WT and IKK β ^{-/-} mice were left untreated or treated with LPS (1 μ g/ml) for 15 minutes, 30 mins, 4 hours or LPS 15 mins and 4 hours + 5 mM ATP (30 min). Cells were then lysed and immunoprecipitated with anti-ASC antibody, followed by western blotting with indicated antibodies. N.D. indicates not detectable, and “UN” indicates left untreated. Data are representative of at least four independent experiments. Error bars represent s.e.m. of technical replicates. * $P < 0.05$ by Mann-Whitney test.

**Figure 8.**

S58 of ASC is a critical residue for IKKi-mediated nuclear-to-cytosolic translocation and inflammasome activation (**a**) HEK 293 cells were transfected with FLAG-IKKi WT or FLAG-IKKi KD, along with either WT ASC or S58A ASC using lipofectamine 2000. Empty vector was used to normalize total plasmid transfected. Cells were then lysed, followed by immunoprecipitation with anti-ASC antibody, and *in vitro* kinase assay. (**b,c**) Immortalized ASC^{-/-} macrophages were retrovirally reconstituted with WT ASC or S58A ASC, then either left untreated, treated with LPS (1 μ g/ml) for 4 hours followed by 5 mM ATP (30 mins), or were transfected with poly(dA:dT) (1.5 μ g/ml) for 4 hours using lipofectamine 2000. Cells were then washed and fixed, and stained with anti-ASC antibody and caspase-1 FLICA (FAM-YVAD-FMK), and images were acquired using confocal microscopy with 60X magnification and 4X enlargement; **scale bars are 5 μ m**. Samples were quantified by counting the number of cells with ASC specks as a percentage of total cells counted in three fields (**b**). Or, lysates were immunoprecipitated with anti-ASC antibody and immunoblotted with the indicated antibodies (**c**). (**d,e**) Immortalized ASC^{-/-} macrophages were retrovirally reconstituted with S193A ASC, S16A ASC, S193A/S58A ASC, or S16A/S58A ASC. Cells were treated with LPS (1 μ g/ml) for 4 hours or with LPS (1 μ g/ml) for 4 hours followed by 5 mM ATP (30 mins). Lysates and supernatants were then collected together and immunoblotted with the indicated antibodies (**d**), or cells were

washed and fixed, stained with anti-ASC antibody and caspase-1 FLICA (FAM-YVAD-FMK), and images were acquired using confocal microscopy with 60X magnification and 4X enlargement; **scale bars are 5 μm** . Samples were quantified by counting the number of cells with ASC specks as a percentage of total cells counted in three fields (e). (f) WT ASC, S58A ASC, S193A/S58A ASC, and S16A/S58A ASC retrovirally reconstituted cells were transfected with poly(dA:dT) (1.5 $\mu\text{g}/\text{ml}$) using lipofectamine 2000 for 4 hours. Lysates and supernatants were then collected together and immunoblotted with the indicated antibodies. “UN” indicates left untreated. Data are representative of at least four independent experiments. Error bars represent s.e.m. of technical replicates. * $P < 0.05$ by Mann-Whitney test.